

Title	Nanoenabling electrochemical sensors for life sciences applications
Authors	Padmanathan, Narayanasamy;Razeeb, Kafil M.;Rohan, James F.;Nagle, Lorraine C.;Wahl, Amélie;Moore, Eric;Messina, Walter;Twomey, Karen;Ogurtsov, Vladimir I.;Galvin, Paul
Publication date	2017-08-14
Original Citation	Galvin, P., Padmanathan, N., Razeeb, K. M., Rohan, J. F., Nagle, L. C., Wahl, A., Moore, E., Messina, W., Twomey, K. and Ogurtsov, V. [2017] 'Nanoenabling electrochemical sensors for life sciences applications', Journal of Materials Research, 32(15), pp. 2883-2904. doi: 10.1557/jmr.2017.290
Type of publication	Article (peer-reviewed)
Link to publisher's version	10.1557/jmr.2017.290
Rights	© Materials Research Society 2017. This article has been published in a revised form in Journal of Materials Research, [http://dx.doi.org/10.1557/jmr.2017.290]. This version is free to view and download for private research and study only. Not for re-distribution, re-sale or use in derivative works.
Download date	2025-03-18 02:11:44
Item downloaded from	https://hdl.handle.net/10468/7635



UCC

University College Cork, Ireland
Coláiste na hOllscoile Corcaigh

Nano-enabling electrochemical sensors for life sciences applications

Paul Galvin*, N. Padmanathan, Kafil M. Razeeb, James F. Rohan, Lorraine C. Nagle, Amelie Wahl, Eric Moore, Walter Messina, Karen Twomey and Vladimir Ogurtsov

Tyndall National Institute, University College Cork, Dyke Parade, Cork, Ireland

* Corresponding author: paul.galvin@tyndall.ie

ABSTRACT

Electrochemical sensing systems are advancing into a wide range of new applications, moving from the traditional lab environment into disposable devices and systems, enabling real-time continuous monitoring of complex media. This transition presents numerous challenges ranging from issues such as sensitivity and dynamic range, to auto-calibration and antifouling, to enabling multiparameter analyte and biomarker detection from an array of nanosensors within a miniaturized form factor. New materials are required not only to address these challenges, but also to facilitate new manufacturing processes for integrated electrochemical systems. This paper examines the recent advances in the instrumentation, sensor architectures and sensor materials in the context of developing the next generation of nano-enabled electrochemical sensors for life sciences applications, and identifies the most promising solutions based on selected well established application exemplars.

I. INTRODUCTION

There are increasing demands for sensing systems that are capable of fast and reliable detection of extremely small quantities of chemical and biochemical targets for applications in environment, security, food safety and medicine. Detection of many of those targets is challenging due to: the complex media in which they are located (i.e. including many interfering species), the high sensitivities and sometimes large dynamic ranges required, the need for the devices to remain functional for extended periods for continuous monitoring applications, the increasingly small form factors of both the instrument and sensor, and the low cost of materials and manufacturing. The challenges of the above user requirements specifications demand a holistic approach to sensor and system development, which includes codesign of the sensor architecture and materials with the instrument. The specification of the sensor materials and design requires a detailed user requirements specification, while the instrument design addresses the specific characteristics of sensor material and configuration. This paper examines the complex issues involved for the development of integrated electrochemical nanosensors for analysis of complex media, and provides an analyses the emerging solutions from the extensive published scientific literature on electrochemical sensors. While electrochemical sensors can, in principle, be fabricated quickly and at low cost, the literature provides a rich source of information on the merits and issues associated with the diverse range of materials, fabrication methods and integration strategies. The main aim of the paper is to deconstruct electrochemical sensor systems into the essential building blocks that are necessary to achieve the user requirements specifications for a given application scenario, including performance, cost, size, number of parameters being measured, etc., and to provide guidance on optimal solutions previously described for each of the required building blocks.

II. INSTRUMENTATION

A. Smart instrumentation for nanosensing technologies

Accurate analyte detection and quantification relies on the chemical sensor behavior resulted from the electron transfer processes between the working electrode and the solution/environment under investigation. This behavior can be complex in particular for electrochemical sensors, where a non-linear diffusion response occurs upon application of a stimulus. The electron transfer which occurs causes a redox chemical reaction whose behavior is governed by Faradays Law and is termed Faradaic Current.¹ This is typically the process that contains the information on the analyte detection/quantification and is described by the following equation.

$$i_F = \frac{dQ}{dt} = \frac{d}{dt}(nFN) = nF \frac{dN}{dt} \quad \text{Eqn 1}$$

Where i_F is the Faradaic current in Amperes, Q is the charge in Coulombs, t is the time in seconds, n is the number of electrons transferred, F is Faradays constant and N is the number of analyte moles transferred.²

However, measurement of this current is complicated by a non-faradaic current component. It is attributed to an electrical double layer capacitance and adsorption/desorption processes which form between the electrode and sensing environment and is governed by Ohms Law.

$$i_{NF} = \frac{V}{Z} \quad \text{Eqn 2}$$

Where i_{NF} is the non-faradaic current in Amps, V is the applied potential in Volts and Z is the electrode impedance in Ohms.

In this process, electrons are not transferred physically across the electrode interface, ions in the solution rearrange themselves to compensate for the charge introduced through the immersion of an electrified electrode in the solution.³ This phenomenon results in the formation of the double layer capacitance, which is made up of the electrical charge at the electrode surface and the ions of opposing charge that are located close to the surface. The double layer capacitance depends on the electrode surface area and structure, analyzed solution composition and applied potential, and can be quite significant. For instance, a typical specific value of this capacitance for a clean platinum surface in contact with 1M aqueous electrolyte solution takes around of 40Fcm^{-2} , thus the double-layer capacitance of a 1 mm radius disk electrode will be approximately 1F.³ The cumulative sensor current will combine both the Faradaic and non-Faradaic responses. Here the capacitance current manifests itself in a surge in current which will mask the Faradaic current of interest. The impact of the non-Faradaic processes can be reduced through use of potentiodynamic techniques that have a pulsing scheme superimposed on the stimulus. Upon application of a pulse, the non-Faradaic charging current component will decay in an exponential manner according to (equation 3) with a time constant $R_u C_{dl}$, where R_u is an uncompensated resistance that arises due to factors such as the inherent resistivity of the analyzed solution, working electrode material and the electrical lead which connects the electrode to the instrumentation⁴ and C_{dl} is the double layer capacitance.

$$i = \frac{E}{R_u} e^{-\frac{t}{R_u C_{dl}}} \quad \text{Eqn 3}$$

The charging current will interfere in the useful signal measurement and reduce the limit of detection. Therefore, this places a stipulation on having a signal measurement at the time that is much greater than double-layer capacitance time constant $R_u C_{dl}$ when the charging current can be negligibly small compared with the Faradaic one. Techniques exist to further reduce the non-Faradaic current impact such as differential pulsed voltammetry whereby current measurement occurs immediately before and after application of a set of voltage pulses. The following sections describe the range of potentiometric and amperometric techniques that are available and widely used with nano-sensors.

B. Impact of a move to nanoscale sensing on the instrumentation requirements

If one considers the trend in reducing the size of the electrode area from macro to micro and, in more recent times, to nanoscale dimensions, consideration must be given to a variety of factors. Wang et al.⁵ have detailed the advantages of miniaturization and highlighted how the capabilities of electrochemistry can be expanded accordingly. Naturally, the current generated at a small scale electrode will be less than that from a larger electrode. This in turn will reduce the size of the Ohmic (iR) drop, which in turn facilitates investigation of highly resistive solutions and also a reduction on the reliance of the supporting electrolyte. With close reference to a reduced double layer capacitance it leads to a smaller $R_u C_{dl}$ time constant and this opens up the ability to carry out high speed voltammetric experiments. A move from planar to radial diffusion associated with transfer from macro to micro sized electrodes in combination with diffusion conduction, occurs at the edge of the small scale electrodes and is commonly termed as ‘edge effects’ leading to enhanced rates of mass transport. This, coupled with the reduced non-Faradaic contribution, results

in the achievement of an increased signal to noise ratio. Such advantages lend themselves to the design of sensors with lower limits of detection of the target analyte, and also to the investigation of solutions that cannot be probed successfully with macro-electrodes, thereby increasing the application scope of electrochemical sensing.

However, reliable measurement of tiny current signals, which requires very small noise and highly sensitive measurement equipment can be performed only in case where the useful signal exceeds the equipment noise levels. Therefore, arrays of nano-electrodes are usually utilized in sensing applications to enhance the signal-to-noise ratio. This is due to the fact that if the useful array signal is proportional to the electrode number N , then the associated array noise is proportional to \sqrt{N} . Careful design of the array is required to achieve full advantages from using of the nano-size array. In the first place, there is a need to ensure that there is no diffusion zone which overlaps from neighboring electrodes, which will result is a change of the conduction mechanism from radial to macro diffusion, and lead to a decrease of the Faradaic current. The usual sensing features of importance include a high repeatability, stability, selectivity and a complete characterization of potential interferents e.g. varying temperature, pH, etc. Also of note is the importance of the reproducibility of the electrode array fabrication. Semiconductor processing techniques, such as those described in this article, allow reliable high volume manufacture of nano-scale electrode arrays. This reproducibility is essential to enable an accurate design file to be generated for the development of instrumentation that will reliably acquire data from the nano-electrodes. To truly take the technology out of the lab environment, the end user will require a plug-and-play approach, whereby a defunct sensor can easily be replaced by a new version with minimal calibration required. In the case where there is only limited batch to batch reproducibility, due perhaps to limitations on the fabrication processes available, correct analyte

detection and quantification based on predefined calibrations will not be feasible; therefore a special sensor calibration procedure will be required from the smart instrumentation.

The instrumentation requirements to a large extent, depend on the requirements of the applications. At the same time they have areas of overlap. To give an example, let us compare the instrumentation requirements for health related and environmental applications. Consider a case of the in-vivo health applications, in which technical requirements such as high miniaturization, continuous powering and reliable and safe wireless communication must be to the forefront. In the case of long-term, reliable sensor monitoring in an unmanned environmental setting e.g. rural water treatment facilities, besides achieving a long life sensor, the instrumentation needs to be autonomous with intelligent/smart operation. Additionally, long-term powering capabilities and communication links with base stations located in some distance from the facility are required for the latter.

The role of the smart chemical sensing system capable of analyte quantification without user intervention is of great importance for emerging Internet of Things (IoT) devices, where they form an essential part of the infrastructure. The concept of the IoT environment is that every object in the Internet Infrastructure (II) is interconnected into a global dynamic expanding network⁶ enabling access to the data of interest. One such object can be a sensor or network of sensors, which communicate wirelessly or via GPRS. These sensor networks find applications in both healthcare and the environment, as well as home and security. There is much activity in reliably connecting wireless sensor networks in the Internet Infrastructure, and the development of a complete sensing system which can be connected in a plug-and-play fashion is a fundamental criterion. Some examples of sensing systems for environmental monitoring include humidity systems with embedded error compensation algorithms to enable accurate measurement⁷,

automated irrigation systems controlled via wireless sensing networks,⁸ air quality monitoring using sensors for carbon monoxide (CO) and volatile organic compounds (VOCs),⁹ water quality monitoring systems.¹⁰⁻¹³

C. Potentiostat Instrumentation

The analytical chemistry methods applied for the separation, identification and quantification of the analytes include static techniques where current does not flow through the solution (potentiometry is the main technique), and dynamic techniques where current flow does occur. Within the dynamic techniques, the electrical parameters of current and potential are controlled, leading to different voltammetric methods such as cyclic voltammetry, pulsed voltammetry, stripping voltammetry, etc. The following is a brief overview of potentiostat instrumentation and recent trends in the technology, where more details can be found from the literature.¹⁴

A potentiostat device serves to apply the voltage across an electrochemical cell (between two electrodes) in accordance to a given value. The effect is achieved by forcing a current into the cell through a third electrode. The invention of the three electrode potentiostat for automatic control of an electrochemical cell was groundbreaking.¹⁵ This and many of the other early potentiostats suffered major problems related to stability. It was not overcome until the field effect transistor was discovered, and the operational amplifier invented, so that the three electrode operational amplifier potentiostat as we know it today was suggested. The first such potentiostat, stable under a wide range of conditions, is attributed to Hans Wenking in 1954. It was central to the creation of the world's first commercial potentiostat manufacturer Bank Elektronik and its core

design remains largely unchanged to this day. In its most basic form, a potentiostat can be implemented using just an operational amplifier (OAMP), and this function is at the core of all potentiostats. Figure 1 displays this fundamental form of a potentiostat acting on a three electrode electrochemical cell.

FIG. 1 near here.

The circuitry represented on the left and on the right is the standard schematic element where such a cell is used. For simplification, the working electrode is grounded; however some current acquisition circuitry will be introduced later. The amplifier will force a current I_{cell} into the solution so that the voltage V_{cell} appears between the reference and working electrodes. The stabilization of the voltage along the reference and the working electrodes V_{RW} around V_{cell} is due to the resistivity of analyte solution between the *RE* and the *CE* electrodes which connects output and non-inverting inputs of the OAMP and thereby loops its feedback. With this arrangement the voltage does not depend on the solution resistivity until the *CE* and OAMP can provide the current required to support V_{cell} . With this, the stability of the voltage applied to *WE* is mostly defined by stability of the reference electrode that makes *RE* a very important part of the three electrode cell.

From a commercial perspective there has been efforts to make modern potentiostats more integrated, miniaturized and with a reduced production cost. Older devices took the form of clunky laboratory units which are expensive and awkward to use. Although some precision devices still take this form, many are much smaller, such as hand held devices or PCMCIA cards. This evolution is illustrated in Figure 2. Improving current sensitivity and dynamic range has also been a priority of modern potentiostats. Current resolutions in the femto-amp range are now reasonable,

for example the Gamry PC14 has a minimum resolution of 2.5fA while being capable of providing full scale current ranges of 7.5nA to 750mA.

FIG. 2. Near here.

From a research perspective, a number of interesting developments and applications have emerged, particularly within the last decade. One of particular interest is the integration of the potentiostat circuitry using CMOS processes, an example of which can be found over two decades ago.¹⁷ This was improved considerably in 1994 when a CMOS device was proposed to include two potentiostat amplifiers (control amplifier and current acquisition amplifier) in addition to DAC for signal generation and ADC for signal acquisition.¹⁸ The current input dual slope ADC offered a minimum resolvable current of 100fA and a maximum of 40mA with a resolution of 13 bits. The device, fabricated with a 2 micron CMOS process, was comparable to much of the commercial electrochemical instrumentation of the time. Its introduction lowered the size, cost and volume of instrumentation, opening up applications in a range of areas.

Following from the numerous developments in potentiostat technology, a number of applications have emerged to take advantage of, in particular smaller and reduced power devices.¹⁹ In-vivo glucose monitoring devices have already been developed where details of those sensor devices discussed later in this paper, and it is expected that an "artificial pancreas" closed-loop system for glucose monitoring and injection of insulin when required will soon be realized. Other investigations of potential potentiostat applications include the use of arrays for electrochemical neural recording.^{20,21} These multichannel potentiostat devices interface with multi-electrode arrays for the sensing of neurotransmitters at a synaptic level. This sensing ability could play a

major role in unravelling the operation of the nervous system, including degenerative disease and response to artificial stimulation. However, current prototypes are typically verified only with in-vitro tests, with progress being made towards a fully integrated and implanted neurotransmitter monitoring systems.

III. BIOIMPEDANCE SENSING

Impedance biosensors based on Electric Cell-substrate Impedance Sensing (ECIS) measure the electrical impedance of an interface in AC steady state with variable frequency, but constant low amplitude (<10 mV) DC bias conditions to avoid disturbing the probe layer, which is an important advantage over voltammetry or amperometry where more extreme voltages are applied.²² ECIS provides an emerging powerful method to perform real time cell monitoring without the use of radioactive tracers, or biological markers. The core of ECIS technology is based on measuring the change in impedance of a small electrode to AC flow. ECIS devices are however not capable of resolving the morphological changes of individual cells within an adhered cell monolayer because the sensors that are used are commonly in the micron range and are based on the inter-digitated electrodes (IDEs) design. IDE's have attracted significant attention in recent years as impedance sensors, due to the hemispherical diffusion, that minimizes convection effects, and the higher sensitivities achievable compared to conventional electrodes in electrochemical measurement. Theoretical calculations²³ predict performance enhancement as dimensions are scaled to sub-micron levels since penetration of the electric field is restricted to the interface region rather than the bulk electrolyte. Typical examples of high resolution array fabrication have been reported by Katz,²⁴ Van Gerwen,²³ Moreno-Hagelsieb,²⁵ among others, with dimensions from 0.25 μm to ~ 1

μm along with various electrical measurement techniques, including microwave resonance detection. The main challenge of impedance biosensor development is the relatively small change of the impedance spectra upon occurrence of the bio-recognition event. The generated signals are especially insignificant when, for example in immunosensors, the antibody concentration is low and the surface coverage of the antigen-antibody complex is far from saturation.²⁴

A range of approaches have been investigated to address the issue of achieving small impedance changes to detect the bio-recognition event. These include amplification via, for example, enzyme labels while the use of nanostructured electrode surfaces modified with nanoparticles²⁶ or carbon nanotubes^{22,27-28} retains the label-free advantages and improves the sensitivity due possibly to significantly enhanced surface area and functionalization. The use of microelectrode arrays has led to unprecedented levels of sensitivity, allowing for example, detection levels for antibodies/antigens at ng/ml, complementary DNA strands at fg/ml levels, and pesticides at 10^{-17} M²⁹. As outlined earlier, there is considerable interest in further reducing the electrode size to sub-micron or nano-scale dimensions to benefit from enlargement of the surface area, projected reduction in capacitance, radial diffusion⁴⁴ and increased mass transport leading to higher current density. Electric field modeling of such arrays has indicated that, as dimensions are reduced, the electric field penetration is restricted to the interface region rather than the bulk electrolyte thus enhanced sensitivity to binding events is likely.^{23,29} Nano-structured sensor designs offer the possibility to overcome the problem of resolving morphological changes of individual cells, and enable an increased signal to noise ratio through minimizing the signal loss due to horizontal electrical conductivity of the electrode. Conventional impedance based sensors to date have relied on micro structured designed electrodes and have proven to be applicable in a wide range of fields.^{31,32} However, with the rapid development of nanotechnology, enabling tools have

emerged where nano-structured electrodes can be fabricated more reproducibly.³³⁻³⁵ The development of nano-structured electrodes for AC impedance measurement offers significant advantages over its micro-structured counterpart. These include, enlargement of the surface area, reduced double layer capacitance, fast convergence to a steady-state signal, better detection limits and increased signal to noise ratios. Another reason why nanostructure electrodes are considered promising is that they offer enhanced current density, that are contributed from increased mass transport at the working electrode interface (Figure 3).

FIG. 3 near here.

ECIS has applications for academic or industrial laboratories in the fields of tissue culture, toxicology, biotechnology, advanced biological methods, regenerative or cell biology. It is a versatile sensitive technique which has also been widely used for interrogating changes at an electrode surface.³⁶ In 1984, Giaever and Keese introduced the ECIS technique for measuring cell-matrix impedance changes as a function of biological processes. When cells are growing in a monolayer, each cell contributes to the impedance signature of the cell-matrix system. They cultured fibroblasts on evaporated gold electrodes and subjected the cell-substrate system to an oscillating electric field. Their results showed that the total impedance of the system depended on cell morphology and cell seeding density on the electrodes. Since then, ECIS has grown to be accepted as a non-invasive technique for monitoring the growth, adhesion, and spreading of mammalian cells in real time.^{31,37-39} Most recently, the technique has been extended to investigate cell migration in wound healing assays,⁴⁰ cell shape change during apoptosis,⁴¹ cell death in

cytotoxicity testing⁴² and the effects of cytoskeleton-disrupting agonists (cytocholasin B) on cell membrane capacitance and intercellular junctional resistance.⁴³

Cell-based biosensors, which treat living cells as sensing elements, are able to detect the functional information of biological active analytes and also provide quantitative analysis. Bioimpedance analysis enables accurate, sensitive and reliable assays to be performed in real time and under constant automated monitoring. These types of biosensors offer the potential to study the behavior of mammalian cells in a non-destructive assay format. Bioimpedance is a measure of the opposition of the flow of an externally applied electric current that is caused by living cells. These systems are measured to give insight into the behavior of cells. Concentration, growth and alterations of the physiological state of cells during cultivation can be detected as impedance changes and thus information about spreading, attachment and morphology of cultured cells can be obtained.^{28,38} The insulating nature of the attached cells, result in a frequency dependent change in the equivalent electrode capacitance. Transcellular and paracellular pathways, originating in either the plasma membrane or the cell adhesion zone together with the intercellular cleft, contribute individual impedance (resistive and capacitive) components which can be determined from their frequency response. The large dielectric dispersions appearing between 10 Hz and tens of MHz (α and β dispersion region) are generally considered to be associated with the diffusion processes of the ionic species (α) and the dielectric properties of the cell membranes and their interactions with the extra and intra-cellular electrolytes (β). The dielectric properties at the gamma region are mostly attributed to the aqueous content of the biological species and the presence of small molecules. The excretion of cellular metabolic products may also be detectable from the electrolyte impedance.³⁰

An advanced technique for transepithelial cell determination was discovered by Wagener and co-workers. They have used ECIS to study the attachment and spreading of epithelial MDCK cells (strain II).³⁸ In impedance measurement, gold electrode was used as an impermeable supports for the cell layers, which in this case, the electrodes were coated with different proteins. A weak AC was supplied between a small working electrode and a large counter electrode, while the voltage was monitored with a lock-in amplifier. The bioimpedance was measured when the cells attached to the electrode were spread.⁴⁴ In addition, ECIS provides a useful description for the cells, in the aspects of conditions and activities of cell culture.

This type of impedance biosensor also can be used to monitor the toxicity in drinking water. Research has been carried out to determine the toxicity in water samples containing 1 of 12 industrial chemicals by comparing the effectiveness of 10 different toxicity sensors, consisted of ECIS, Eclox, Hepatocyte low density lipoprotein (LDL) uptake, Microtox, Mitoscan, Neuronal microelectrode array, Sinorhizobium meliloti toxicity test, SOS cytosensor system, Toxi-Chromotest and ToxScreen II.⁴⁵ The results showed that combination of ECIS with another two different sensors (Microtox and the Hepatocyte LDL uptake test) provide greater sensitivity in chemicals detection of 9 out of 12 chemicals. Other than cytotoxicity studies, ECIS also can be used in drug development. In 2004, Arndt and co-workers have developed an electrochemical technique of ECIS to monitor the apoptosis-induced changes in biological activity independent of the trigger mechanism in a strictly physiological environment.⁴¹ It has been proven that the sensor is significantly more sensitive compared to caspase-3 activity or structural changes in the cell-cell contacts. Therefore, the continued evolution of patterning and modification technologies to achieve more reproducible nanostructured surfaces has enabled the advancement of transducers with a particular focus on label-free sensing.

IV ONE DIMENSIONAL NANOSTRUCTURED SENSOR ARRAYS

A. Glucose sensors

Since the invention in 1960's, the glucose biosensor developed rapidly, and currently occupies approximately 85% of the entire biosensor market.⁴⁶ Besides blood glucose measurement, glucose biosensors are also widely used in bio industrial process monitoring, quality control, fuel cells and, particularly in medical applications.⁴⁷ Accordingly, most research and development has been devoted in this area. From clinical aspects, diabetes mellitus is one of the leading causes of death and disability in the world.⁴⁶⁻⁴⁸ Generally, insulin deficiency and hyperglycemia varies the blood glucose concentrations in the normal range of about 3.9–6.2 (empty stomach) or 3.9–7.8 (2 h after having food) mM.⁴⁹ Therefore, quantitative monitoring of blood glucose is of great clinical importance, in order to reduce the risks of diabetes mellitus induced heart disease, kidney failure, or blindness.^{49,50} In addition to glucose, hydrogen peroxide (H_2O_2) is necessary for the metabolism of proteins, carbohydrates, fats, vitamins, and minerals.^{51,52} Besides its essential role for the production of estrogens, progesterone, and thyroxin in the body, H_2O_2 helps regulate blood glucose and cellular energy production. Oxidative damages in the body are caused by cellular H_2O_2 imbalance as this chemical plays an important role in cell signaling and communication.⁵² Therefore, the detection of H_2O_2 also has a significance and importance like the glucose biosensor in the biomedical chemistry.

Electrochemical glucose sensors have been categorized into two types based on enzymatic sensing and the non-enzymatic sensing. The sensor systems sensitivity (i.e. linear range of analyte response) and selectivity (i.e. the ratio between analyte of interest and a particular interference) are the two important parameters for assessing the analytical reliability of the device. Therefore,

improvements in sensitivity and selectivity of the sensors have always been of paramount interest.⁵³ To date many reviews have been published which distinguished the various aspects of both enzyme and non-enzyme based biosensors. Wang, Heller and Feldman have briefly addressed the importance and trends of enzymatic glucose sensors towards diabetes management.^{46,47} Park et al reviewed the principle and clear perspective of non-enzymatic glucose sensors.^{54,55} Si et al reviewed the recent development of nano-materials for the application of electrochemical non-enzymatic glucose biosensors.⁵⁶ However, some important aspects on this topic have not been sufficiently addressed in the literature. This deficiency is especially true of those of based on metal/metal oxide nanowire-nanoparticle electro catalysts for electrochemical biosensors. It is well known that the nanostructured electrocatalysts promise to solve issues associated with the enzymatic and non-enzymatic electrodes such as instability, poor selectivity, and surface fouling, while nano-materials-based non-enzymatic biosensors show significantly higher sensitivity than enzymatic systems.⁵⁶ Thus, an understanding of nanostructured electrocatalysts, and their complete surface reaction mechanism towards biochemical reactions during sensing is necessary to make reliable devices. As a result of their unique features, one-dimensional nanostructures (i.e. especially nanowires) have attracted much attention due to their potential use as interconnects in fabricating electronic devices.^{57,58} Therefore, here we review the present state of the art for the 1D nanowire/nanoparticle based metal/metal oxide electrocatalysts for glucose and H₂O₂ detection using enzyme and non-enzymatic systems. We also review the potential for emerging nano-porous gold substrates to provide enhanced sensing performance.

Since dimensionality plays a key role in materials properties, significant experimental efforts have focused on producing one dimensional nano-crystals or nanowires.⁵⁷⁻⁶¹ Hence, a wide range of transition metal nano-materials have been studied in recent years for the electrocatalytic

biosensing. In particular of Gold (Au), Silver (Ag), Palladium (Pd), Platinum (Pt), Copper (Cu), Nickel (Ni) and their combinations are the widely investigated materials for biosensors. Here we discuss the 1D nanowire/nanoparticle based electrocatalyst for both enzymatic and non-enzymatic biosensors.

One dimensional transition metal nanowire array electrodes have demonstrated excellent performance for the electrochemical biosensors.⁶² Nanowires with the unique catalytic activities and electronic properties are widely used to improve sensitivity and selectivity of the electrochemical biosensors, facilitate electron transfer, and decrease overpotential. The excellent properties of nanowires are due to several beneficial features arising from their shape anisotropy on the electrochemical reaction at electrodes: (i) facile pathways for the electron transfer by reducing the number of interfaces between the nanoparticle catalysts and (ii) effective surface exposure to work as active catalytic sites in the electrode–electrolyte interface.⁶³⁻⁶⁵ Due to their unique dimensionality and large surface area, enzymes can be adsorbed onto these 1D nanostructures.⁶⁶ Since Clark and Lyons proposed in 1962 the initial concept of glucose enzyme electrodes, a tremendous effort has been directed to develop reliable biosensors with enzyme based electrodes. Although commercially available glucose sensing devices are dominated by enzymatic systems, in the last decade there is an increased research interest in non-enzymatic biosensors.

B. Enzymatic Glucose sensors

Glucose Oxidase (GOx) is the ideal enzyme and widely used in the majority of commercial biosensors, great effort has been devoted towards the improvement of GOx-based biosensors.⁶⁷ Chen et al. described recent advances in electrochemical glucose biosensors and focused on some problems and bottlenecks in areas of enzymatic (glucose oxidase (GOx) based) amperometric

glucose sensing⁴⁹. Herein recent achievements in this area have focused on the development of novel nanowire electrocatalyst and the study of direct electron transfer with the assistance of functional nano-materials. Wang et al reported an amperometric glucose biosensor based on silver nanowires and GOx.⁶⁸ The biosensor showed the linear range from the 0.01 to 0.8 mM with a detection limit of 2.3 μM (S/N = 3). Wang et al fabricated a novel glucose biosensor based on the immobilization of GOx onto gold nanoparticles-modified Pb nanowires.⁶⁹ The synergistic effect of Pb nanowires and gold nanoparticles made the biosensor exhibit excellent electrocatalytic activity and good response towards glucose. The biosensor showed the sensitivity of 135.5 $\mu\text{A mM}^{-1} \text{cm}^{-2}$, the detection limit of 2 μM (S/N = 3), and the response time <5 s with a linear range of 0.005–2.2 mM. Lu et al investigated enzyme-functionalized gold nanowires for the fabrication of glucose biosensors and achieved the response time of <8 s, a linear range of 0.01 – 20 mM and detection limit of 5 μM .⁷⁰ Delvaux and Champagne reported the arrays of nanoscopic gold tubes for glucose sensor and reached the glucose response as large as 0.4 $\mu\text{A mM}^{-1} \text{cm}^{-2}$ in presence of GOx.⁷¹ Claussen et al fabricated porous anodic alumina templated Au/GOx nanoarray electrode on silicon chip for glucose sensor. The sensitivity to glucose is controlled by manipulating the length and composition of the immobilized GOx-conjugated self-assembled monolayers (SAMs). This controllable shift in glucose sensitivity and likewise linear sensing range allows biosensor development for specific applications.⁷² Similarly, Wen et al developed a biosensor with Pt-CNT-GOx which exhibits a good linear relationship with the concentration of glucose in the range of 0.16–11.5 mM; the regression equation with the calibration plot is $C \text{ (mM)} = 0.16I \text{ (I is current response)} + 2.05$ with a correlation coefficient of 0.994 (n = 12). The response time for the successive addition of glucose was about 5 s, and the detection limit was determined to be 0.55 μM glucose based on S/N = 3.⁷³ Meantime, Liu et al presented the direct electron transfer between

GOx in carbon decorated ZnO nanowire array electrode for glucose biosensor. With subsequent successive addition of glucose, the biosensor showed the fast response time of ~5s with 0.01 – 1.6 mM glucose response range.⁷⁴ It is well accepted that at the nanoscale regime, the properties of materials strongly influenced by their shape and dimensionality. Therefore, it is interesting to fabricate nanostructured material with different textural features including nanowires and nanorods and to examine its intrinsic characteristic for use in electrochemical glucose sensors. Because of their high surface to volume ratio with the unique structure and shape, these one dimensional nanostructures (e.g. nanowires) will allow rapid electron transfer and hence enhances the catalytic response towards glucose detection. Figure 4 showed the SEM images of metal/metal oxide nanowire and nanorod structure reported earlier.

FIG. 4 near here.

Table 1 near here.

Pradhan et al demonstrated the light-weight flexible glucose sensor bioelectrode based on the ZnO nanowires directly deposited on Au-coated PET substrate. Using an amperometric method, the GOx/ZnO-NWs/Au/PET bioelectrode is found to exhibit excellent and fast glucose sensing performance, with a high sensitivity of $19.5 \mu\text{A mM}^{-1} \text{cm}^{-2}$ and a low Michaelis-Menten constant of 1.57 mM, making ZnO NW-based biosensors promising candidates for future commercialization.⁷⁵ A range of recent electrodes based on one dimensional nanostructure and their electrochemical glucose detection mechanisms in the presence of the GOx are compared in Table 1.

C. Non-enzymatic Glucose sensors

In spite of the low detection limit, enzymatic glucose sensors are constrained by a number of factors, including: stability issues that originated from the nature of the enzymes⁵⁴; limited selectivity for glucose detection in blood samples; and the high operating potential required during the measurements can result in interference associated with the presence of other electro active species such as ascorbic acid (AA), acetaminophen (AC) and uric acid (UA).⁸⁸ Therefore, non-enzymatic glucose sensors are highly desirable based on the direct oxidation of glucose on the electrode surface without using the fragile enzyme. Enzyme-less glucose sensors are expected to have advantages such as simplicity, reproducibility, good stability, and free from oxygen limitation.⁵⁴ To date various metals and metal oxides have been explored for non-enzymatic glucose detection and detailed review articles have been published.⁵⁴⁻⁵⁶ Therefore in this review, we have focused mainly on the benefit to non-enzymatic glucose sensors of one dimensional metal/metal oxide nanostructures, and in particular of nanowire architectures.

It has been reported that Au electrodes can display high electrocatalytic activity toward the oxidation of glucose, and many methods of fabricating Au nanowire array electrodes have been explored. Yang et al described the fabrication of network film electrodes with ultrathin Au nanowires for non-enzymatic glucose sensing. The network film electrode biosensor fabricated with 2 nm Au NWs exhibits high sensitivity ($56.0 \mu\text{A cm}^{-2} \text{mM}^{-1}$), low detection limit ($20 \mu\text{M}$), short response time (within 10s), excellent selectivity, and good storage stability for a non-enzymatic glucose sensor.⁸⁹ Cherevko and Chung reported a gold nanowire array electrode for non-enzymatic voltammetric and amperometric glucose detection.⁹⁰ The wide dynamic range and high sensitivity, selectivity and stability, as well as good biocompatibility of the Au NW electrode make it promising for the fabrication of non-enzymatic glucose sensors. The amperometric

detection was shown within the physiologically important range of glucose concentration, with a very high sensitivity of $309.0 \mu\text{A mM}^{-1} \text{cm}^{-2}$. In advance, Zhao et al invented the facile multistep approach to fabricate Au nanowire array electrode and demonstrated for non-enzymatic glucose sensor. They have integrated three techniques i.e. vacuum sputtering-deposition, holographic photo-lithography and argon ion beam etching to prepare efficient Au nanowire electrodes.⁹¹ The biosensor showed a linear amperometric response to the oxidation of glucose in a concentration range of 0.4 – 10 mM. Other work reported by Bai et al, describes the direct electrodeposition of Pt-Pb nanowire array electrode as an enzyme-free glucose sensor.⁹² To effectively avoid the interference coming from ascorbic acid, a negative potential of -0.20 V was chosen for glucose detection, and the sensitivity of the sensor to glucose oxidation was $11.25 \mu\text{A mM}^{-1} \text{cm}^{-2}$ with linearity up to 11 mM, and a detection limit of 8 μM (signal-to-noise ratio of 3). Similar metal/metal oxide nanowire architectures and their catalytic performance for glucose biosensors have been compared with the values tabulated in Table 2.

Table 2 near here

In transition metals, the Ni has showed better electrocatalytic activity owing to their strong $\text{Ni}^{2+}/\text{Ni}^{3+}$ and widely investigated for non-enzymatic glucose sensors. Recently, the Ni nanowire strategies have received great interest for biosensors. Liu et al designed a nano-Ni based ultrasensitive non-enzymatic electrochemical glucose sensor via a nanowire array strategy.⁹⁶ Jamal et al explored the Ni nanowire array and Pt-decorated Ni nanowire array electrode for an enzyme-free glutamate sensor,⁹⁷ and the same group have extended their work with Ni/NiO core-shell nanowire array electrodes for non-enzymatic glucose sensors. Interestingly, both Ni and

NiO@Ni nanowires array electrodes exhibit excellent electro-catalytic activity, and the sensitivity of NiNAE and NiO@NiNAE has been found to be 80.0 and 170.4 $\mu\text{A mM}^{-1} \text{cm}^{-2}$, respectively. Under optimal detection conditions, the as-prepared sensors exhibited linear behavior for glucose detection in the concentration up to 7 mM for both NiNAE and NiO@NiNAE with a limit of detection of 33 and 14 μM , respectively.⁹⁸

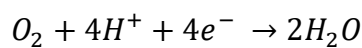
FIG. 5 near here.

It is interesting to note that the formation of the reaction intermediate NiOOH in the case of NiO is one step less compared to Ni, which is the rate determining step for the glucose oxidation. Furthermore, it is found that NiO is a good catalyst and thus the electro-catalytic behavior completely dominates the capacitive behavior in the presence of glucose and the current response is completely due to the electro-oxidation of glucose. Therefore, the surface oxidation of Ni nanowires can be an excellent electrocatalytic material for the detection of glucose. In continuation, Sherdedani et al demonstrated a prickly Ni nanowire array grown on Cu substrate as a supersensitive glucose biosensor in the absence of enzymes.⁹⁹ Figure 5(a-d) shows the SEM images of Ni nanowire array electrode for biosensors fabricated using different techniques. In other aspects, Zhang et al¹⁰⁰ developed the Cu nanowire electrode for ultrasensitive and selective non-enzymatic glucose detection, where the amperometric detection of glucose using the Cu NWs modified glassy carbon electrode exhibited a limit of detection of just 35 nM while retaining a wide dynamic range. The reported sensitivity of 420.3 $\mu\text{A mM}^{-1} \text{cm}^{-2}$, was more than 10,000 times higher than that of the control electrode without Cu NWs. Ruimin Ding et al reported mixed Ni-

Cu nanowire array electrodes for enzyme free glucose sensor, which yielded a detection limit of 0.1 μM , a linear range of 0.0001–1.2 mM and sensitivity as high as 1600 $\mu\text{A mM}^{-1} \text{cm}^{-2}$.¹⁰⁴

D. Hydrogen peroxide (H_2O_2) biosensor

Hydrogen peroxide (H_2O_2) can exert detrimental effects on biological systems and contribute to the neuropathology of central nervous system diseases.¹¹¹ It also plays a significant role in the production and fate of hydroxyl and peroxyhydroxyl radicals in the troposphere.¹¹² Because the determination of H_2O_2 is also very important in enzymatic reactions, the trace determination of H_2O_2 is of considerable importance in clinical and environmental applications.¹¹³ Glucose detecting by biosensors usually involves two steps of chemical reactions as follows:⁴⁶



At first, the immobilized GOx converts glucose and oxygen into gluconic acid and H_2O_2 ; second, H_2O_2 is oxidized to O_2 when a working potential is applied to the biosensor. An electric current proportional to glucose concentration is measured to quantify glucose.¹¹⁴ Hence, H_2O_2 sensing plays an essential role in the determination of the blood glucose content but is also important in dyes, food, as well as pharmaceutical industries.

Table 3 near here.

As for glucose, the electrochemical detection of H_2O_2 could be classified into enzymatic detection and non-enzymatic detection. Because of the unique selectivity as well as high sensitivity, enzyme-based biosensors have been widely applied for the H_2O_2 determination. A

significant amount of work in enzyme based biosensors is related to the detection of H_2O_2 , a co-product of enzymatic oxidation using oxidases have been reported. However, they may suffer from stability issues, limited lifetime and a complex fabrication procedure. While non-enzymatic H_2O_2 sensors have attracted increasing interest, the electrochemical reaction of H_2O_2 on bare electrodes often encounters interferences from common coexisting species in the absence of enzyme. Recently, some non-enzymatic H_2O_2 sensors have been proposed based on metal and transition metal oxide materials-modified electrodes; herein we have focused on the 1D nanostructure, in particular nanowire array electro-catalysts for non-enzymatic H_2O_2 biosensors. Hsiao et al reported the first case of using urchin like Ag NWs for non-enzymatic H_2O_2 sensing.¹¹⁵ The Ag NW electrode shows that its sensitivity for H_2O_2 reduction at an applied potential -0.28 V in PBS is $4705 \mu\text{A mM}^{-1} \text{cm}^{-2}$ with the detection limit of $10 \mu\text{M}$. Meantime, Kurowska et al investigated the silver nanowire array sensor for sensitive and rapid detection of H_2O_2 .¹¹⁶ The fabricated Ag NW array H_2O_2 sensor showed high sensitivity of about $2.66 \mu\text{A mM}^{-1} \text{cm}^{-2}$ and wide range of response from 0.1 mM to 3.1 mM with a detection limit of $29.2 \mu\text{M}$. The developed Ag NW array sensor excluded the interference from substances typically present in the biological samples such as ascorbic acid (AA), uric acid (UA), ethanol (EtOH), glucose (G) and oxalate ions. In advance, Li et al developed a new strategy to grow seed mediated Au long nanowires for high performance H_2O_2 sensors.¹¹⁷ They have used three steps to fabricate long Au nanowires i.e. amino modification of SiO_2 nanospheres, Au seed loading and subsequently seed mediated nanowire growth. Moreover, they found that as-prepared non-enzymatic H_2O_2 sensor based on Au NWs exhibit enhanced catalytic performance such as a high and wide range of sensitivity with a lower detection limit when compared to Au nanoparticles. In other work, Jamal et al fabricated Pd-modified gold nanowire array electrodes as a highly sensitive H_2O_2 sensor.¹¹⁸ Typical amperometric H_2O_2 sensors

showed a linear response up to 2 mM of H₂O₂ with a sensitivity of 530 $\mu\text{A mM}^{-1} \text{cm}^{-2}$ at 20 °C. This electrode can detect 5 μM (S/N = 3) of H₂O₂ at normal conditions without using any enzyme or mediator. In addition, Huang et al demonstrated improved performance of non-enzymatic H₂O₂ detection with CuO particle decorated Si nanowires.¹¹⁹ Interestingly, the CuO assembled on silicon nanowires (CuO/SiNWs) showed a competent sensitivity of 22.3 $\mu\text{A/mM}^{-1}$, a wider linear range from 0.01 to 13.2mM, and a comparable detection limit of 1.6 μM (3 S/N) for non-enzymatic H₂O₂ detection. Furthermore, our recent work on horseradish peroxidase (HRP) modified Au nanowire array electrode demonstrated excellent H₂O₂ detection with high sensitivity and selectivity,¹²⁰ where the designed H₂O₂ sensor showed a sensitivity of 45.9 $\mu\text{A mM}^{-1} \text{cm}^{-2}$, with the 0.42 μM detection limit, and wide range of linearity up to 15 mM. Table 3 provides a summary of reports on horseradish peroxidase based enzymatic H₂O₂ sensors and of recent works with different metal/metal oxide 1D nanostructures for enzymatic and non-enzymatic H₂O₂ sensors including a comparison of their catalytic performances.

E. Features of 1D Nanostructure Array Strategy in electro-catalytic performances

Sensitivity and Selectivity

One of the major challenges in glucose and H₂O₂ biosensors could be electrochemically active interferents, which generate electrochemical signals at the same potential as glucose. Usually, the ground subtraction method is used to eliminate signals generated due to ascorbic acid (AA) and uric acid (UA), which are common electrochemical interferents in physiological fluid. However, it was observed that the nanowire/nanorod based 1D array strategy can provide novel and augmented functionality to minimize the electrochemical interferent elements in both enzymatic and non-enzymatic biosensors systems. According to Qu et al, the current generated due to the interferences 0.1 mM (AA), 0.1 mM (UA), and 1 mM (acetaminophen) are negligible

when compared to glucose response indicating high selectivity of the biosensors.^[20] Furthermore, the sensitivity of the electrode remained relatively constant for first 20 days followed by 85% after one month. Recently, Hsu et al verified the selectivity of Au–Ni coaxial nanorod array electrode to sequential injections of 5.5 mM glucose, 5 mM uric acid (UA), 5 mM ascorbic acid (AA), and 5.5 mM glucose in an oxygen-containing PBS solution.⁷⁶ They found that Au-Ni nanorod array electrode biosensor is free from the common interferences and showed the 5.5 mM glucose detection even after 30 days.

FIG. 6 near here.

Similarly, the case studies of non-enzymatic biosensors also showed the excellent selectivity and sensitivity performance. For example, the Ni nanowire array electrode fabricated by our group for glucose biosensors reported negligible interference.⁹⁸ In presence of 1 mM glucose, 100 μ M uric acid, 100 μ M ascorbic acid, 140 μ M acetaminophen and 1 μ M dopamine, the yielded current response was only ranging from 5–7%. In another work, the same group further revealed the very low interference of UA and AA with the Pt-Ni NWs array electrode.⁹⁷ Furthermore, typical current response curves of Pt-Ni NWs and NiO@Ni NWs array electrode in the presence of various interferences are shown in Figure 6(a and b)., Jamal and coworkers further investigated the selectivity of a Pd-decorated Au nanowire array as a H₂O₂ sensor.¹¹⁸ They found that only 1-3% of the current was obtained for common interferences such as AA and UA, and negligible current responses for the other acetaminophen and dopamine interferents. These results are encouraging and strongly support a novel nanowire array strategy for further augmentation of biosensors in application sectors such as clinical, food, pharmaceutical and environmental industries.

V. NANOPOROUS METALS FOR ELECTROCHEMICAL SENSING.

A highly active form of metal catalyst has been developed in recent years based on nanoporous metals which can be formed by additive or subtractive processes. In particular the demonstration of a simple process for nanoporous metal fabrication by a chemical etching process called dealloying or selective metal dissolution has spurred investigations of the potential applications of such materials. Dealloying is not a new process and had a cosmetic use in ancient Incan civilization whereby a dealloying process was used to create an illusion of pure Au by depletion gilding of Cu-Au alloy surfaces.

The field of nanoporous materials has only relatively recently been developed based on some early corrosion studies and observations using electron microscopy. Pickering and Swann¹²⁹ examined Cu-Au, Cu-Al, Cu-Zn and Mg-Al alloys and concluded that compositional variations led to preferential chemical attack at grain boundaries on the surface of the alloys studied. Pickering and Wagner¹³⁰ investigated the dealloying process and proposed the dissolution process is most active at kink-step-terrace sites analogous to metal vaporization.

In 1979, Forty¹³¹ used transmission electron microscope (TEM) images to demonstrate that for such depletion gilding of a less-noble metal from AuAg alloys, selective dissolution in nitric acid during anodic corrosion results in a continuous open nanoporous structure composed almost entirely of Au. Thus the less noble Ag species is selectively dissolved not only at the surface of the alloy but also to an appreciable depth. He surmised that mass transport of atoms is occurring either through the bulk of the crystal lattice or across the surface to support the continuing dissolution. Surface diffusion of Au as the surface Ag atoms dissolve from the Au_xAg_y alloy leads to reformed Au-rich islands, so that fresh Ag atoms are continuously exposed to the environment

layer by layer to create a rough surface eventually leading to an evolved nanoporous gold (NPG) material.

More recent studies have identified the requirements for optimized NPG formation together with theoretical interpretations of the structural evolution process which typically involves alloys of Ag, Cu and Al and results in nanoporous materials with differing porosity and composition. Al and Cu can passivate during the dealloying process leaving a non-negligible concentration of Al and Cu within the NPG. The more commonly used AuAg alloy is a single face centered cubic crystal phase that can be dealloyed to > 99 percent¹³² and the resulting porous structure is homogenous throughout the entire material. The difference in the standard electrochemical potential of the alloy metals constituents is used to achieve nanoporosity during the chemical etch. It has also been shown that for a particular composition in excess of 55% Ag, and at a given overpotential to drive the reaction, the desired nanoporosity can be induced in the Au.

Erlebacher and co-workers¹³³⁻¹³⁸, have probed and identified the conditions necessary and proposed a supporting theory for NPG formation involving electrochemical dissolution of the less noble metal in the alloy, surface diffusion of the more noble material and finally capillary action which results in coarsening of the structure and the emergence of filaments of the nanoporous material. Porosity evolution in NPG proposed by Erlebacher et al begins by dissolution of a the less noble metal atom from an initially flat terrace which is the rate-determining step that determines the energetics of dissolution. As a vacancy island grows laterally, the neighboring atoms of the first terrace vacancy dissolve away. The Au atoms have sufficiently high diffusion rates along step edges and move with the receding vacancy island into gold-rich islands which are further undercut as more layers are dissolved forming the uppermost layer of ligaments.

Annealing the formed nanoporous materials can induce further coarsening of the ligaments.¹³⁹⁻¹⁴⁰ Indeed the ligament and pore sizes can be decreased by:

- (i) increasing the Ag content of the alloy precursor
- (ii) Increasing the dealloying potential
- (iii) decreasing electrolyte temperature¹⁴¹
- (iv) Post-treatment in acid¹⁴²

In general the sponge-like 3D structure is a system of interconnecting nanopores / tunnels in a skeleton of nanofilaments of the metal. This bicontinuous structure has a number of unique characteristics that result in properties that can be exploited for a wide range of applications. The filament size can range from 5-50 nm and surface areas as high as 20 m² g⁻¹ with a porosity of 70 % or higher are possible. Au is second only to Ag in terms of electronic conductivity and as such the interconnected filaments of NPG also possess this key conduction and interconnect or homogeneity advantage over dispersed catalyst nuclei or alternative metals on lower conductivity catalyst supports. SEM and TEM images of NPG formed from an alloy of AuAg in nitric acid are shown in Figure 7 with typical ligament and pore dimensions.

NPG is mechanically far stronger than expected on the basis of a scaling law, presumably given that the ligament size in the nm range which causes dislocation starvation. Biener et al¹⁴³ noted one of the surprising aspects of NPG is that it brings together the apparently conflicting properties of high strength and high porosity. They characterized the size-dependent mechanical properties of NPG using a combination of nanoindentation, column microcompression and molecular dynamics simulations. They concluded that NPG can be as strong as bulk Au, despite being a highly porous material, and that its ligaments approach the theoretical yield strength of Au.

FIG. 7 near here.

De Hosson and co-workers¹⁴⁴ exploited the ability to alter the pore size in the fabrication of dual length-scale NPG by controlling the grain structure of the alloy precursor. They demonstrated that the two length-scale structure enhances the functional properties of nanoporous gold, leading to charge-induced strains of amplitude up to 6%, which are roughly two orders of magnitude larger than in nanoporous Au with the standard single length-scale porous morphology. A further exploitation of the mechanically enhanced NPG materials has been demonstrated by Oppermann et al.¹⁴⁵ They utilized NPG as the top surface on a Si chip bump for electronic interconnection. In flip chip bonding they found that flip chip bonding could be achieved at low temperature and with low force bonding conditions. The porous interconnects have very promising properties, like compressibility and reduced stiffness, which are required for advanced microelectronic manufacturing leading to higher bond yield and extended reliability.

This form of Au contains an intrinsically high step density. Given that NPG has an interconnected, bicontinuous ligament network containing regions of both negative and positive curvature, a high step density is topologically required. This characteristic makes NPG attractive for catalysis studies. It is made even more attractive because it can be easily formed into thin, high-conductivity foils that are easily adapted to electrocatalytic measurements.

In terms of catalytic applications, NPG has at least two advantages over other catalysts including Au nanoparticles. Firstly, unlike well-established Pt or Pd catalysts, NPG remains active at low temperature (room temperature or even lower), which is desirable for many practical applications. Secondly, NPG has a good thermal stability, is resistant to oxidation¹⁴⁶ and thus can overcome the aggregation or sintering limitations from which Au nanoparticles often suffer at higher temperatures or in an oxidative environment.¹⁴⁷

The development of processes for the formation of and the theoretical understanding of NPG has coincided with the emerging field of gold catalysis and electrocatalysis as researchers demonstrate applications for what had until the mid-1980's been considered a poor catalyst material. The observations of Hutchings¹⁴⁸ that Au³⁺ could catalyze the hydrochlorination of acetylene and Haruta¹⁴⁹ that nanosized Au the oxidation of carbon monoxide far below room temperature demonstrated the potential use of Au as a catalyst. Subsequent analysis has

highlighted that the properties of the bulk metal do not govern its catalytic properties and that highly reactive surface Au species dominate. Previously, the filled d-band for Au and its well-recognized poor chemisorption properties limited studies of Au to fundamental or baseline studies to probe chemical or electrochemical reactions in the absence of a catalytic response. A number of examples have been reported of catalytic reactions involving NPG consistent with the overall hypothesis that the central difference between NPG and bulk Au is due to the increased density of step edges in NPG over bulk Au. CO Oxidation at low temperature over unsupported NPG was shown by Xu et al.¹⁵⁰ NPG in a foam type structure has been shown to exhibit high CO oxidation activity.¹⁵¹ NPG has been shown to be an effective catalyst for reduction of hydrogen peroxide to water.¹⁵² Zhang et al reported that NPG shows much higher electrocatalytic activity towards methanol than polycrystalline Au.¹⁵³ Wittstock et al¹³² demonstrated selectivity levels in excess of 97 % for gas-phase oxidative coupling of methanol to methyl formate at temperatures below 80 °C with high turnover frequencies which is required in practical applications. Glucose oxidation with high electrocatalytic activity at NPG was shown by Deng et al.¹⁵⁴

At the Tyndall National Institute, we have recently investigated borane and borohydride oxidation reactions at gold electrodes, examples of the linear sweep voltammograms are shown in Figures 8 (a) and (b). The onset potential for both borane¹⁵⁵ and borohydride¹⁵⁶ oxidation at NPG (blue curve) was shifted to more negative potentials than that observed at a Au disc (red curve) and higher currents were realized. An onset potential for oxidation more than 200 mV closer to the standard redox potential was recorded at NPG by comparison with bulk or even nanowires of Au. The rate of reaction was up to 23 times higher at NPG than at a bulk Au disc electrode. The initiation of the oxidation reaction at such a low overpotential is indicative of the high activity of the surface sites at the NPG substrate. The difference between the electrochemical outputs of the Au nanowires (green curve) formed by template electrodeposition in porous alumina (ca. 200 nm diameter) and the 20 nm ligaments of NPG indicate that a significant advantage is gained by decreasing the dimension of the nanomaterial for electrocatalytic reactions.

FIG. 8 near here.

A similarly enhanced response to hydrazine oxidation at NPG has been observed by Liu et al.¹⁵⁷ The onset of hydrazine oxidation had an overpotential decrease of 200 mV by comparison with bulk Au. In that study a lower detection limit for hydrazine in PBS of 16.7 nM was achieved. While this limit is lower than a number of other sensor materials investigated such as carbon nanotubes or Cu-Pd nanoparticles, it did not surpass citrate stabilized Au nanoparticles for which the detection limit is 200 pM.¹⁵⁸ A similarly enhanced response (by 200 mV) at NPG for hydrogen peroxide sensing by comparison with bulk Au in PBS at a pH of 7 has also been reported.¹⁵⁹ They showed that the NPG exhibits good selectivity with respect to potential interferents in real biological samples, such as, methanol, ethanol, glucose and ascorbic acid.

The enhanced electrocatalytic properties of NPG have also been investigated for a number of sensing applications, by incorporation of the NPG onto micro-disc arrays, including those with integrated reference and counter electrodes as low cost alternatives to single standard micro-disc electrodes. The arrays were fabricated at the Tyndall National Institute using standard silicon microfabrication techniques of metal and dielectric materials deposition, followed by patterning with photoresists and finally dicing into individual chips for packaging and electrochemical testing. Recessed gold microelectrode arrays were modified with NPG by electrodepositing a gold-silver alloy therein and selectively dissolving the silver component. Arrays of recessed gold micro-band electrodes (17 electrodes in an array, width 10 μm , length 500 μm , inter-electrode spacing 100 μm and recess 730 nm) and recessed gold micro-disc electrodes (314 electrodes in an array, diameter 10 μm , inter-electrode spacing 100 μm and recess 917 nm) modified with 473 nm and 252 nm NPG, respectively are shown in Figure 9. The thickness of the NPG was controlled by the deposition time of the precursor gold-silver alloy. The electrochemically active surface area of the micro-band array increased 14-fold upon modification with NPG.

An example of the output has been reported recently for an NPG modified microelectrode array fabricated at the Tyndall National Institute.^{160,161} The array was utilized for oxygen detection in water samples to analyse drinking water quality in rural India where the advantages of low cost miniaturized systems are apparent. The NPG modified micro-disc array outperformed by more than two fold the unmodified Au disc array, in terms of both the signal to noise ratio and the response time which help to facilitate remote sample analysis.

FIG. 9 near here

Recently NPG has been utilized as a biocompatible neural interface coating.¹⁶² The authors demonstrated that NPG facilitates close physical coupling of neurons by maintaining a high neuron-to-astrocyte surface coverage ratio. They highlighted that the topography, reduces astrocyte surface coverage while maintaining high neuronal coverage and may enhance neuron–electrode coupling through nanostructure-mediated suppression of scar tissue formation.

Nanoporous materials other than Au have also been investigated and the processing and mechanism established in detail for Au are being utilized to develop nanoporous metals and alloys for various applications. Examples include nanoporous Pt which can be fabricated from an alloy of Cu.¹⁶³ The authors dealloyed Cu from $\text{Cu}_{0.75}\text{Pt}_{0.25}$ alloy in 1M H_2SO_4 . They achieved porosity with a diameter of approximately 3.4 nm. The small pore size was attributed to the extremely small values of surface diffusivity expected for Pt at room temperature. The results also showed that larger length scales can be achieved through coarsening at elevated temperatures. Nanoporous Cu¹⁶⁴ has also been achieved by the selective corrosion of single-phase $\text{Cu}_{30}\text{Mn}_{70}$ alloy in HCl

aqueous solutions. For applications where high conductivity, low cost conductors or as supports for active materials such a nanoporous material may prove to be a valuable candidate.

Nanoporous Ru¹⁶⁵ has also been fabricated from Ru_{0.20}Mn_{0.80} alloy for CO oxidation. The authors achieved NPRu by dealloying or selective dissolution of manganese (Mn) from RuMn alloy having investigated a number of other alloying metals such as Co, Ni, Fe, Cr and Ti. The pore size and specific surface area of fabricated NPRu were 3 nm and 51.5m² g⁻¹ respectively. They found that the NPRu was active to CO oxidation. XPS analysis did indicate that the surface was oxidized with a thin layer of ruthenium oxide which is expected based on the known ease with which nanoscale Ru can be oxidised by the ambient. Chen and Sieradzki utilized the same principles to develop a process for nanoporous Sn¹⁶⁶ by dissolution of a lithium alloy in an acetonitrile water mixture. The authors found that at concentrations of the order of 50 at.% Li, bicontinuous porosity was achieved and that at Li concentrations larger than 75 at.% the nanostructure similar to that of NPG was evident. This opens up a wide range of alternative materials that can benefit from nanoporosity by dealloying in non-aqueous solvents for controlled dissolution leading to a continuous ligament of the metal or alloy. In this case the authors investigated Sn as a potential anode material for advanced lithium batteries. Sn has three times the energy density of typical Li-ion battery carbon anodes, however, like a number of potential high energy density anode materials such as Al, Ge and Si it suffers significant volume expansion during Li intercalation which leads to pulverization and loss of active material on cycling. Having a route to a continuous electrically connected network which can be microns in thickness but with porosity and thus amenable to volume expansion is a significant development. The initial results presented in this work show an improved lithium battery electrode performance with the potential for improvement.

The developments presented above show that novel routes to and applications of nanoporous materials has developed at a significant rate over the past decade. The extremely reactive and stable surface particularly in the case of the most studied NPG has led to its use in a variety of applications and its use as a sensor is of particular interest. The combination of nanoporosity and placement of active materials on micro or nanoelectrode arrays opens the possibility for the deployment of many sensors based on the combined advantages of Au and nanoporosity which include;

- Bicontinuous network of interconnecting, tunable pores in a skeleton of Au ligaments
- High surface to volume ratio
- Pores 15 nm, ligaments 20-40 nm
- Specific surface area $4 \text{ m}^2 \text{ g}^{-1}$
- Pore volume $0.005 \text{ cm}^3 \text{ g}^{-1}$
- Biocompatibility
- High strength material
- High step density-catalytically active sites
- Chemical and thermal stability

Additional applications such as enhanced bonding materials for electronic devices or as active electrode materials for next generation energy storage devices such as batteries, fuel cells or supercapacitors could see further integration of materials functions for energy, electronics and sensing which are key issues in the deployment of distributed sensors or Things in the rapidly developing Internet of Things.

CONCLUSIONS

Electrochemical sensing platforms are rapidly transforming from the conventional single use, in vitro diagnostic scenarios to continuous monitoring with complex media for health, biotech and environmental monitoring applications. Real-time continuous monitoring not only presents challenges associated with biofouling and sensor calibration, but in the case of wearable, minimally invasive, implantable or process monitoring devices used in the food or pharmaceutical/biopharmaceutical industries, biocompatibility of the sensing materials is a prerequisite. While glucose sensing from fresh blood at physiological levels has not been technically challenging with respect to the sensitivities required, many of the analytes and biomarkers of importance for monitoring health and wellness do require sensitivities beyond today's state of the art performance (e.g. nucleic acid and protein biomarkers for early detection of cancer or testing for drugs¹⁶⁷). The combination of emerging sensing platforms and electronic instrumentation promises not only to address those sensitivity issues, but to enable complete sensing solutions. These whole systems will need to provide multiparameter sensing within low cost miniaturized form factors, compatible with integration on wearable technologies, surgical tools, minimally invasive implantable devices and inline process analytical monitoring. Extended shelf-life stability and auto-calibration will be critical for most applications, but will be especially challenging in the case of biochemical sensors, particularly those involving enzymes as part of their sensing modality. Power consumption and power management will also be critical success factors for enabling autonomous electrochemical sensor systems to capture the right data at the right time; this will require intelligent control systems that adapt measurement protocols based on embedded software analysis of the data collected, appropriately managing the delicate balance between energy expenditure incurred by data communication with subsequent data processing in the cloud, versus local processing (with more limiting processing power) which could reduce the required frequency

of data communication. With the development of high-volume low-cost miniaturized integrated circuits compatible with integration at or near the sensor, and in some cases as a single solid state device, it is increasingly possible to integrate high sensitivity multiparameter nanosensor arrays with signal processing electronics, to minimize issues with data quality between the sensor and the electronics. Sensor manufacture is also evolving rapidly, in terms of the materials used (e.g. increasing use of flexible electronics), the manufacturing processes involved (e.g. additive manufacturing) and the overall move towards automation of biomedical device manufacturing in line with Industry 4.0.

In summary, with the many opportunities for leveraging innovative nano-enabled electrochemical sensors into new life sciences applications, it is important to ensure that resources are efficiently used, leveraging the significant experience gained over the last decades on electrochemical sensor development.

ACKNOWLEDGEMENTS

The authors would like to acknowledge financial support from Science Foundation Ireland, Enterprise Ireland, European Commission FP6, FP7 and H2020 Programs.

REFERENCES

1. E.J. Calvo: Chapter 1 Fundamentals. The Basics of Electrode Reactions, in *Comprehensive Chemical Kinetics*, edited by C. H. Bamford and R. G. Compton (Elsevier, City, 1986), pp. 1.
2. M. Ciobanu, J.P. Wilburn, M.L. Krim and D.E. Cliffel: 1 - Fundamentals, in *Handbook of Electrochemistry*, edited by C. G. Zoski (Elsevier, City, 2007), pp. 3.
3. R.L. William and P.O. Mark: Voltammetry, in *Analytical Instrumentation Handbook*, Third Edition, (CRC Press, City, 2004), pp. 529.
4. J.C. Myland and K.B. Oldham: Uncompensated Resistance. 1. The Effect of Cell Geometry *Analytical Chemistry*. **72**(17), 3972 (2000).
5. J. Wang: *Analytical electrochemistry* (John Wiley & Sons, City, 2006).
6. M.S. Farash, M. Turkanovic, S. Kumari and M. Holbi: An efficient user authentication and key agreement scheme for heterogeneous wireless sensor network tailored for the Internet of Things environment *Ad Hoc Networks*. **36**, 152 (2016).
7. K. Arshak, K. Twomey, D. Heffernan, Ieee and Ieee: Development of a novel humidity sensor with error-compensated measurement system, in *2002 23rd International Conference on Microelectronics*, Vols 1 and 2, Proceedings, (City, 2002), pp. 215.
8. K.I. Arshak and K. Twomey: Investigation into a novel humidity sensor operating at room temperature *Microelectronics Journal*. **33**(3), 213 (2002).

9. C. Goumopoulos, B. O'Flynn and A. Kameas: Automated zone-specific irrigation with wireless sensor/actuator network and adaptable decision support *Computers and Electronics in Agriculture*. **105**, 20 (2014).
10. V.I. Ogurtsov, K. Twomey and G. Herzog: Development of an Integrated Electrochemical Sensing System to Monitor Port Water Quality Using Autonomous Robotic Fish, in *Comprehensive Materials Processing*, edited by S. H. F. B. J. V. T. Yilbas (Elsevier, City, 2014), pp. 317.
11. Lawlor, J. Torres, B. O'Flynn, J. Wallace and F. Regan: DEPLOY: a long term deployment of a water quality sensor monitoring system *Sensor Review*. **32**(1), 29 (2012).
12. G. Herzog, W. Moujahid, K. Twomey, C. Lyons and V.I. Ogurtsov: On-chip electrochemical microsystems for measurements of copper and conductivity in artificial seawater *Talanta*. **116**, 26 (2013).
13. K. Twomey, E.A. de Eulate, J. Alderman and D. Arrigan: Fabrication and characterization of a miniaturized planar voltammetric sensor array for use in an electronic tongue *Sensors and Actuators B: Chemical*. **140**(2), 532 (2009).
14. K. Twomey, L. Nagle, A. Said, F. Barry and V. Ogurtsov: Characterisation of Nanoporous Gold for Use in a Dissolved Oxygen Sensing Application *BioNanoScience*. **5**(1), 55 (2015).
15. C.M. Caffrey, O. Chevalerias, C.O. Mathuna and K. Twomey: Swallowable-capsule technology *Pervasive computing, IEEE*. **7**(1), 23 (2008).
16. Hickling: Studies in electrode polarisation. Part IV. - The automatic control of the potential of a working electrode *Transactions of the Faraday Society*. **38**, 27 (1942).

17. Mc Caffrey: Development of Circuitry and Software for a Diagnostic Swallowable Capsule, in Department of Microelectronics and Tyndall National Institute, UCC, (University College Cork, City, 2008), p. 216.
18. R.F.B. Turner, D.J. Harrison and H.P. Baltes: A CMOS potentiostat for amperometric chemical sensors *Solid-State Circuits, IEEE Journal of.* **22**(3), 473 (1987).
19. R.J. Reay, S.P. Kounaves and G.T.A. Kovacs: An integrated CMOS potentiostat for miniaturized electroanalytical instrumentation, in Solid-State Circuits Conference, 1994. Digest of Technical Papers. 41st ISSCC., 1994 IEEE International, (City, 1994), pp. 162.
20. Bandyopadhyay, G. Mulliken, G. Cauwenberghs and N. Thakor: VLSI potentiostat array for distributed electrochemical neural recording, in Circuits and Systems, 2002. ISCAS 2002. IEEE International Symposium on, (2, City, 2002), pp. II.
21. K. Murari, N. Thakor, M. Stanacevic and G. Cauwenberghs: Wide-range, picoampere-sensitivity multichannel VLSI potentiostat for neurotransmitter sensing, in Engineering in Medicine and Biology Society, 2004. IEMBS '04. 26th Annual International Conference of the IEEE, (2, City, 2004), pp. 4063.
22. J. Galandova, G. Ziyatdinova and J. Labuda: Disposable electrochemical biosensor with multiwalled carbon nanotubes - Chitosan composite layer for the detection of deep DNA damage *Analytical Sciences.* **24**(6), 711 (2008).
23. P. Van Gerwen, W. Laureyn, W. Laureys, G. Huyberechts, M.O. De Beeck, K. Baert, J. Suls, W. Sansen, P. Jacobs, L. Hermans and R. Mertens: Nanoscaled interdigitated electrode arrays for biochemical sensors *Sens. Actuator B-Chem.* **49**(1-2), 73 (1998).

24. E. Katz and I. Willner: Probing biomolecular interactions at conductive and semiconductive surfaces by impedance spectroscopy: Routes to impedimetric immunosensors, DNA-Sensors, and enzyme biosensors *Electroanalysis*. **15**(11), 913 (2003).
25. L. Moreno-Hagelsieb, B. Foutier, G. Laurent, R. Pampin, J. Remacle, J.P. Raskin and D. Flandre: Electrical detection of DNA hybridization: Three extraction techniques based on interdigitated Al/Al₂O₃ capacitors *Biosensors & Bioelectronics*. **22**(9-10), 2199 (2007).
26. J.S. Daniels and N. Pourmand: Label-free impedance biosensors: Opportunities and challenges *Electroanalysis*. **19**(12), 1239 (2007).
27. J.E. Trancik, S.C. Barton and J. Hone: Transparent and catalytic carbon nanotube films *Nano Letters*. **8**(4), 982 (2008).
28. Y. Yun, R. Gollapudi, V. Shanov, M.J. Schulz, Z.Y. Dong, A. Jazieh, W.R. Heineman, H.B. Halsall, D.K.Y. Wong, A. Bange, Y. Tu and S. Subramaniam: Carbon nanotubes grown on stainless steel to form plate and probe electrodes for chemical/biological sensing *Journal of Nanoscience and Nanotechnology*. **7**(3), 891 (2007).
29. K.A. Law and S.P.J. Higson: Sonochemically fabricated acetylcholinesterase micro-electrode arrays within a flow injection analyser for the determination of organophosphate pesticides *Biosensors & Bioelectronics*. **20**(10), 1914 (2005).
30. Z.W. Zou, J.H. Kai, M.J. Rust, J. Han and C.H. Ahn: Functionalized nano interdigitated electrodes arrays on polymer with integrated microfluidics for direct bio-affinity sensing using impedimetric measurement *Sensors and Actuators a-Physical*. **136**(2), 518 (2007).
31. E. Moore, O. Rawley, T. Wood and P. Galvin: Monitoring of cell growth in vitro using biochips packaged with indium tin oxide sensors *Sens. Actuator B-Chem*. **139**(1), 187 (2009).

32. L. Ceriotti, A. Kob, S. Drechsler, J. Ponti, E. Thedinga, P. Colpo, R. Ehret and F. Rossi: Online monitoring of BALB/3T3 metabolism and adhesion with multiparametric chip-based system *Analytical Biochemistry*. **371**(1), 92 (2007).
33. W. Hu, A.S. Crouch, D. Miller, M. Aryal and K.J. Luebke: Inhibited cell spreading on polystyrene nanopillars fabricated by nanoimprinting and in situ elongation *Nanotechnology*. **21**(38), (2010).
34. W. Messina, M. Fitzgerald, E. Moore: SEM and ECIS investigation of cells cultured on nanopillar modified interdigitated impedance electrodes for analysis of cell growth and cytotoxicity of potential anticancer drugs *Electroanalysis* **2016**, 28, 2188-2195.
35. J. Lee, M.J. Cuddihy and N.A. Kotov: Three-dimensional cell culture matrices: State of the art *Tissue Engineering Part B-Reviews*. **14**(1), 61 (2008).
36. I.D. Raistrick, D.R. Franceschetti and J.R. Macdonald: Theory Impedance Spectroscopy: Theory, Experiment, and Applications, 2nd Edition. 27 (2005).
37. Giaever and C.R. Keese: Micromotion of Mammalian-Cells measured Electrically *Proceedings of the National Academy of Sciences of the United States of America*. **88**(17), 7896 (1991).
38. J. Wegener, C.R. Keese and I. Giaever: Electric cell-substrate impedance sensing (ECIS) as a noninvasive means to monitor the kinetics of cell spreading to artificial surfaces *Experimental Cell Research*. **259**(1), 158 (2000).
39. S. Belkin: Microbial whole-cell sensing systems of environmental pollutants *Current Opinion in Microbiology*. **6**(3), 206 (2003).

40. C.R. Keese, J. Wegener, S.R. Walker and L. Giaever: Electrical wound-healing assay for cells in vitro *Proceedings of the National Academy of Sciences of the United States of America*. **101**(6), 1554 (2004).
41. S. Arndt, J. Seebach, K. Psathaki, H.J. Galla and J. Wegener: Bioelectrical impedance assay to monitor changes in cell shape during apoptosis *Biosensors & Bioelectronics*. **19**(6), 583 (2004).
42. C. Xiao and J.H.T. Luong: Assessment of cytotoxicity by emerging impedance spectroscopy *Toxicology and Applied Pharmacology*. **206**(2), 102 (2005).
43. D. Opp, B. Wafula, J. Lim, E. Huang, J.C. Lo and C.M. Lo: Use of electric cell-substrate impedance sensing to assess in vitro cytotoxicity *Biosensors & Bioelectronics*. **24**(8), 2625 (2009).
44. C.E. Campbell, M.M. Laane, E. Haugarvoll and I. Giaever: Monitoring viral-induced cell death using electric cell-substrate impedance sensing *Biosensors & Bioelectronics*. **23**(4), 536 (2007).
45. W.H. van der Schalie, R.R. James and T.P. Gargan: Selection of a battery of rapid toxicity sensors for drinking water evaluation *Biosensors & Bioelectronics*. **22**(1), 18 (2006).
46. J. Wang: Electrochemical Glucose Biosensors *Chem. Rev.* **108**(2), 814 (2008).
47. A. Heller and B. Feldman: Electrochemical Glucose Sensors and Their Applications in Diabetes Management *Chem. Rev.* **108**(7), 2482 (2008).
48. K. Tian, M. Prestgard and A. Tiwari: A review of recent advances in nonenzymatic glucose sensors *Materials Science and Engineering: C*. **41**, 100 (2014).

49. C. Chen, Q. Xie, D. Yang, H. Xiao, Y. Fu, Y. Tan and S. Yao: Recent advances in electrochemical glucose biosensors: a review *RSC Advances*. **3**(14), 4473 (2013).
50. J. Hu: The evolution of commercialized glucose sensors in China *Biosens. and Bioelect.* **24**(5), 1083 (2009).
51. W. Dröge: Free Radicals in the Physiological Control of Cell Function *Physiological Reviews*. **82**(1), 47 (2002).
52. M.M. Rahman, A.J.S. Ahammad, J.-H. Jin, S.J. Ahn and J.-J. Lee: A Comprehensive Review of Glucose Biosensors Based on Nanostructured Metal-Oxides *Sensors*. **10**(5), 4855 (2010).
53. C.I.L. Justino, T.A. Rocha-Santos, A.C. Duarte and T.A. Rocha-Santos: Review of analytical figures of merit of sensors and biosensors in clinical applications *TrAC Trends in Analytical Chemistry*. **29**(10), 1172 (2010).
54. S. Park, H. Boo and T.D. Chung: Electrochemical non-enzymatic glucose sensors *Analytica Chimica Acta*. **556**(1), 46 (2006).
55. K.E. Toghill and R.G. Compton: Electrochemical non-enzymatic glucose sensors: a perspective and an evaluation *Int J Electrochem Sci*. **5**(9), 1246 (2010).
56. P. Si, Y. Huang, T. Wang and J. Ma: Nanomaterials for electrochemical non-enzymatic glucose biosensors *RSC Advances*. **3**(11), 3487 (2013).
57. Y. Xia, P. Yang, Y. Sun, Y. Wu, B. Mayers, B. Gates, Y. Yin, F. Kim and H. Yan: One-dimensional nanostructures: synthesis, characterization, and applications *Advanced materials*. **15**(5), 353 (2003).
58. E.P. Lee, J. Chen, Y. Yin, C.T. Campbell and Y. Xia: Pd-Catalyzed Growth of Pt Nanoparticles or Nanowires as Dense Coatings on Polymeric and Ceramic Particulate Supports *Advanced Materials*. **18**(24), 3271 (2006).

59. Y. Sun and Y. Xia: Large-scale synthesis of uniform silver nanowires through a soft, self-seeding, polyol process *Nature*. **353**(1991), 737 (1991).
60. T. Hanrath and B.A. Korgel: Supercritical fluid–liquid–solid (SFLS) synthesis of Si and Ge nanowires seeded by colloidal metal nanocrystals *Advanced Materials*. **15**(5), 437 (2003).
61. Z.L. Wang: Nanowires and Nanobelts: Materials, Properties and Devices. Volume 1: Metal and Semiconductor Nanowires (Springer Science & Business Media, City, 2013).
62. V. Anandan, Y.L. Rao and G. Zhang: Nanopillar array structures for enhancing biosensing performance *International journal of nanomedicine*. **1**(1), 73 (2006).
63. H. Wang, X. Wang, X. Zhang, X. Qin, Z. Zhao, Z. Miao, N. Huang and Q. Chen: A novel glucose biosensor based on the immobilization of glucose oxidase onto gold nanoparticles-modified Pb nanowires *Biosensors and Bioelectronics*. **25**(1), 142 (2009).
64. F. Qu, M. Yang, G. Shen and R. Yu: Electrochemical biosensing utilizing synergic action of carbon nanotubes and platinum nanowires prepared by template synthesis *Biosensors and Bioelectronics*. **22**(8), 1749 (2007).
65. S.M. Choi, J.H. Kim, J.Y. Jung, E.Y. Yoon and W.B. Kim: Pt nanowires prepared via a polymer template method: its promise toward high Pt-loaded electrocatalysts for methanol oxidation *Electrochimica Acta*. **53**(19), 5804 (2008).
66. N.S. Birenbaum, B.T. Lai, C.S. Chen, D.H. Reich and G.J. Meyer: Selective noncovalent adsorption of protein to bifunctional metallic nanowire surfaces *Langmuir*. **19**(23), 9580 (2003).
67. R. Wilson and A. Turner: Glucose oxidase: an ideal enzyme *Biosensors and Bioelectronics*. **7**(3), 165 (1992).

68. L. Wang, X. Gao, L. Jin, Q. Wu, Z. Chen and X. Lin: Amperometric glucose biosensor based on silver nanowires and glucose oxidase *Sensors and Actuators B: Chemical*. **176**, 9 (2013).
69. Y. Lu, M. Yang, F. Qu, G. Shen and R. Yu: Enzyme-functionalized gold nanowires for the fabrication of biosensors *Bioelectrochemistry*. **71**(2), 211 (2007).
70. M. Delvaux and S. Demoustier-Champagne: Immobilisation of glucose oxidase within metallic nanotubes arrays for application to enzyme biosensors *Biosensors and Bioelectronics*. **18**(7), 943 (2003).
71. J.C. Claussen, M.M. Wickner, T.S. Fisher and D.M. Porterfield: Transforming the fabrication and biofunctionalization of gold nanoelectrode arrays into versatile electrochemical glucose biosensors *ACS applied materials & interfaces*. **3**(5), 1765 (2011).
72. Z. Wen, S. Ci and J. Li: Pt nanoparticles inserting in carbon nanotube arrays: nanocomposites for glucose biosensors *The Journal of Physical Chemistry C*. **113**(31), 13482 (2009).
73. J. Liu, C. Guo, C.M. Li, Y. Li, Q. Chi, X. Huang, L. Liao and T. Yu: Carbon-decorated ZnO nanowire array: a novel platform for direct electrochemistry of enzymes and biosensing applications *Electrochemistry Communications*. **11**(1), 202 (2009).
74. D. Pradhan, F. Niroui and K. Leung: High-performance, flexible enzymatic glucose biosensor based on ZnO nanowires supported on a gold-coated polyester substrate *ACS applied materials & interfaces*. **2**(8), 2409 (2010).
75. C.-W. Hsu and G.-J. Wang: Highly sensitive glucose biosensor based on Au–Ni coaxial nanorod array having high aspect ratio *Biosensors and Bioelectronics*. **56**, 204 (2014).
76. X. Yang, Y. Wang, Y. Liu and X. Jiang: A sensitive hydrogen peroxide and glucose biosensor based on gold/silver core–shell nanorods *Electrochimica Acta*. **108**, 39 (2013).

77. Z. Yang, Y. Tang, J. Li, Y. Zhang and X. Hu: Facile synthesis of tetragonal columnar-shaped TiO₂ nanorods for the construction of sensitive electrochemical glucose biosensor *Biosensors and Bioelectronics*. **54**, 528 (2014).
78. Y. Xie and W. Wang: Bioelectrocatalytic performance of glucose oxidase/nitrogen-doped titania nanotube array enzyme electrode *Journal of Chemical Technology and Biotechnology*. (2015).
79. K. Qu, P. Shi, J. Ren and X. Qu: Nanocomposite Incorporating V₂O₅ Nanowires and Gold Nanoparticles for Mimicking an Enzyme Cascade Reaction and Its Application in the Detection of Biomolecules *Chemistry-A European Journal*. **20**(24), 7501 (2014).
80. Y. Wei, Y. Li, X. Liu, Y. Xian, G. Shi and L. Jin: ZnO nanorods/Au hybrid nanocomposites for glucose biosensor *Biosensors and Bioelectronics*. **26**(1), 275 (2010).
81. X. Liu, Q. Hu, Q. Wu, W. Zhang, Z. Fang and Q. Xie: Aligned ZnO nanorods: a useful film to fabricate amperometric glucose biosensor *Colloids and Surfaces B: Biointerfaces*. **74**(1), 154 (2009).
82. K. Yang, G.-W. She, H. Wang, X.-M. Ou, X.-H. Zhang, C.-S. Lee and S.-T. Lee: ZnO nanotube arrays as biosensors for glucose *The Journal of Physical Chemistry C*. **113**(47), 20169 (2009).
83. J. Zang, C.M. Li, X. Cui, J. Wang, X. Sun, H. Dong and C.Q. Sun: Tailoring zinc oxide nanowires for high performance amperometric glucose sensor *Electroanalysis*. **19**(9), 1008 (2007).
84. X. Jia, G. Hu, F. Nitze, H.R. Barzegar, T. Sharifi, C.-W. Tai and T. Wågberg: Synthesis of Palladium/Helical Carbon Nanofiber Hybrid Nanostructures and Their Application for

- Hydrogen Peroxide and Glucose Detection *ACS applied materials & interfaces*. **5**(22), 12017 (2013).
85. D. Patil, N.Q. Dung, H. Jung, S.Y. Ahn, D.M. Jang and D. Kim: Enzymatic glucose biosensor based on CeO₂ nanorods synthesized by non-isothermal precipitation *Biosensors and Bioelectronics*. **31**(1), 176 (2012).
86. Z. Wang, S. Liu, P. Wu and C. Cai: Detection of glucose based on direct electron transfer reaction of glucose oxidase immobilized on highly ordered polyaniline nanotubes *Analytical Chemistry*. **81**(4), 1638 (2009).
87. K.K. Lee, P.Y. Loh, C.H. Sow and W.S. Chin: CoOOH nanosheets on cobalt substrate as a non-enzymatic glucose sensor *Electrochemistry Communications*. **20**, 128 (2012).
88. L. Yang, Y. Zhang, M. Chu, W. Deng, Y. Tan, M. Ma, X. Su, Q. Xie and S. Yao: Facile fabrication of network film electrodes with ultrathin Au nanowires for nonenzymatic glucose sensing and glucose/O₂ fuel cell *Biosensors and Bioelectronics*. **52**, 105 (2014).
89. S. Cherevko and C.-H. Chung: Gold nanowire array electrode for non-enzymatic voltammetric and amperometric glucose detection *Sensors and Actuators B: Chemical*. **142**(1), 216 (2009).
90. Y. Zhao, J. Chu, S.H. Li, W.W. Li, G. Liu, Y.C. Tian and H.Q. Yu: Non-Enzymatic Electrochemical Detection of Glucose with a Gold Nanowire Array Electrode *Electroanalysis*. **26**(3), 656 (2014).
91. Y. Bai, Y. Sun and C. Sun: Pt–Pb nanowire array electrode for enzyme-free glucose detection *Biosensors and Bioelectronics*. **24**(4), 579 (2008).

92. S.S. Mahshid, S. Mahshid, A. Dolati, M. Ghorbani, L. Yang, S. Luo and Q. Cai: Template-based electrodeposition of Pt/Ni nanowires and its catalytic activity towards glucose oxidation *Electrochimica Acta*. **58**, 551 (2011).
93. J. Yuan, K. Wang and X. Xia: Highly Ordered Platinum-Nanotubule Arrays for Amperometric Glucose Sensing *Advanced Functional Materials*. **15**(5), 803 (2005).
94. Y. Li, X. Niu, J. Tang, M. Lan and H. Zhao: A Comparative Study of Nonenzymatic Electrochemical Glucose Sensors Based on Pt-Pd Nanotube and Nanowire Arrays *Electrochimica Acta*. **130**, 1 (2014).
95. L.-M. Lu, L. Zhang, F.-L. Qu, H.-X. Lu, X.-B. Zhang, Z.-S. Wu, S.-Y. Huan, Q.-A. Wang, G.-L. Shen and R.-Q. Yu: A nano-Ni based ultrasensitive nonenzymatic electrochemical sensor for glucose: enhancing sensitivity through a nanowire array strategy *Biosensors and Bioelectronics*. **25**(1), 218 (2009).
96. M. Jamal, M. Hasan, A. Mathewson and K.M. Razeeb: Disposable sensor based on enzyme-free Ni nanowire array electrode to detect glutamate *Biosensors and Bioelectronics*. **40**(1), 213 (2013).
97. M. Jamal, M. Hasan, M. Schmidt, N. Petkov, A. Mathewson and K.M. Razeeb: Shell@ Core coaxial NiO@ Ni nanowire arrays as high performance enzymeless glucose sensor *Journal of The Electrochemical Society*. **160**(11), B207 (2013).
98. R.K. Shervedani, M. Karevan and A. Amini: Prickly nickel nanowires grown on Cu substrate as a supersensitive enzyme-free electrochemical glucose sensor *Sensors and Actuators B: Chemical*. **204**, 783 (2014).

99. Y. Zhang, L. Su, D. Manuzzi, H.V.E. de los Monteros, W. Jia, D. Huo, C. Hou and Y. Lei: Ultrasensitive and selective non-enzymatic glucose detection using copper nanowires *Biosensors and Bioelectronics*. **31**(1), 426 (2012).
100. Z.D. Gao, J. Guo, N.K. Shrestha, R. Hahn, Y.Y. Song and P. Schmuki: Nickel Hydroxide Nanoparticle Activated Semi-metallic TiO₂ Nanotube Arrays for Non-enzymatic Glucose Sensing *Chemistry-A European Journal*. **19**(46), 15530 (2013).
101. K. Huo, Y. Li, R. Chen, B. Gao, C. Peng, W. Zhang, L. Hu, X. Zhang and P.K. Chu: Recyclable Non-Enzymatic Glucose Sensor Based on Ni/NiTiO₃/TiO₂ Nanotube Arrays *ChemPlusChem*. **80**(3), 576 (2015).
102. C. Wang, L. Yin, L. Zhang and R. Gao: Ti/TiO₂ nanotube array/Ni composite electrodes for nonenzymatic amperometric glucose sensing *The Journal of Physical Chemistry C*. **114**(10), 4408 (2010).
103. R. Ding, J. Liu, J. Jiang, J. Zhu and X. Huang: Mixed Ni–Cu-oxide nanowire array on conductive substrate and its application as enzyme-free glucose sensor *Analytical Methods*. **4**(12), 4003 (2012).
104. M. Long, L. Tan, H. Liu, Z. He and A. Tang: Novel helical TiO₂ nanotube arrays modified by Cu₂O for enzyme-free glucose oxidation *Biosensors and Bioelectronics*. **59**, 243 (2014).
105. S. Yu, X. Peng, G. Cao, M. Zhou, L. Qiao, J. Yao and H. He: Ni nanoparticles decorated titania nanotube arrays as efficient nonenzymatic glucose sensor *Electrochimica Acta*. **76**, 512 (2012).
106. J. Huang, Y. Zhu, X. Yang, W. Chen, Y. Zhou and C. Li: Flexible 3D porous CuO nanowire arrays for enzymeless glucose sensing: in situ engineered versus ex situ piled *Nanoscale*. **7**(2), 559 (2015).

- 107.J. Wang, W. Bao and L. Zhang: A nonenzymatic glucose sensing platform based on Ni nanowire modified electrode *Analytical Methods*. **4**(12), 4009 (2012).
- 108.X. Cao and N. Wang: A novel non-enzymatic glucose sensor modified with Fe₂O₃ nanowire arrays *Analyst*. **136**(20), 4241 (2011).
- 109.Z. Zhuang, X. Su, H. Yuan, Q. Sun, D. Xiao and M.M. Choi: An improved sensitivity non-enzymatic glucose sensor based on a CuO nanowire modified Cu electrode *Analyst*. **133**(1), 126 (2008).
- 110.E.A. Mazzio and K.F. Soliman: Glioma cell antioxidant capacity relative to reactive oxygen species produced by dopamine *Journal of Applied Toxicology*. **24**(2), 99 (2004).
- 111.Y. Komazaki, T. Inoue and S. Tanaka: Automated measurement system for H₂O₂ in the atmosphere by diffusion scrubber sampling and HPLC analysis of Ti (IV)–PAR–H₂O₂ complex *Analyst*. **126**(5), 587 (2001).
- 112.X. Shu, Y. Chen, H. Yuan, S. Gao and D. Xiao: H₂O₂ sensor based on the room-temperature phosphorescence of nano TiO₂/SiO₂ composite *Analytical chemistry*. **79**(10), 3695 (2007).
- 113.F. Wang, X. Liu, C.-H. Lu and I. Willner: Cysteine-mediated aggregation of Au nanoparticles: the development of a H₂O₂ sensor and oxidase-based biosensors *ACS nano*. **7**(8), 7278 (2013).
- 114.W.H. Hsiao, H.Y. Chen, T.M. Cheng, T.K. Huang, Y.L. Chen, C.Y. Lee and H.T. Chi: Urchin-like Ag Nanowires as Non-enzymatic Hydrogen Peroxide Sensor *Journal of the Chinese Chemical Society*. **59**(4), 500 (2012).
- 115.E. Kurowska, A. Brzózka, M. Jarosz, G. Sulka and M. Jaskuła: Silver nanowire array sensor for sensitive and rapid detection of H₂O₂ *Electrochimica Acta*. **104**, 439 (2013).

116. Y. Li, L. Zu, G. Liu, Y. Qin, D. Shi and J. Yang: Nanospherical Surface-Supported Seeded Growth of Au Nanowires: Investigation on a New Growth Mechanism and High-Performance Hydrogen Peroxide Sensors *Particle & Particle Systems Characterization*. **32**(4), 498 (2015).
117. M. Jamal, M. Hasan, A. Mathewson and K.M. Razeeb: Non-enzymatic and highly sensitive H₂O₂ sensor based on Pd nanoparticle modified gold nanowire array electrode *Journal of The Electrochemical Society*. **159**(11), B825 (2012).
118. J. Huang, Y. Zhu, H. Zhong, X. Yang and C. Li: Dispersed CuO Nanoparticles on a Silicon Nanowire for Improved Performance of Nonenzymatic H₂O₂ Detection *ACS applied materials & interfaces*. **6**(10), 7055 (2014).
119. J. Xu, F. Shang, J.H. Luong, K.M. Razeeb and J.D. Glennon: Direct electrochemistry of horseradish peroxidase immobilized on a monolayer modified nanowire array electrode *Biosensors and Bioelectronics*. **25**(6), 1313 (2010).
120. W. Bai, J. Zheng and Q. Sheng: A Non-Enzymatic Hydrogen Peroxide Sensor Based on Ag/MnOOH Nanocomposites *Electroanalysis*. **25**(10), 2305 (2013).
121. F. Meng, X. Yan, J. Liu, J. Gu and Z. Zou: Nanoporous gold as non-enzymatic sensor for hydrogen peroxide *Electrochimica Acta*. **56**(12), 4657 (2011).
122. L. Wang, M. Deng, G. Ding, S. Chen and F. Xu: Manganese dioxide based ternary nanocomposite for catalytic reduction and nonenzymatic sensing of hydrogen peroxide *Electrochimica Acta*. **114**, 416 (2013).
123. S. Su, X. Wei, Y. Guo, Y. Zhong, Y. Su, Q. Huang, C. Fan and Y. He: A Silicon Nanowire-Based Electrochemical Sensor with High Sensitivity and Electrocatalytic Activity *Particle & Particle Systems Characterization*. **30**(4), 326 (2013).

- 124.X. Pang, D. He, S. Luo and Q. Cai: An amperometric glucose biosensor fabricated with Pt nanoparticle-decorated carbon nanotubes/TiO₂ nanotube arrays composite *Sensors and Actuators B: Chemical*. **137**(1), 134 (2009).
- 125.Q. Kang, L. Yang and Q. Cai: An electro-catalytic biosensor fabricated with Pt–Au nanoparticle-decorated titania nanotube array *Bioelectrochemistry*. **74**(1), 62 (2008).
- 126.B.X. Gu, C.X. Xu, G.P. Zhu, S.Q. Liu, L.Y. Chen, M.L. Wang and J.J. Zhu: Layer by Layer Immobilized Horseradish Peroxidase on Zinc Oxide Nanorods for Biosensing *The Journal of Physical Chemistry B*. **113**(18), 6553 (2009).
- 127.A.K.M. Kafi, G. Wu and A. Chen: A novel hydrogen peroxide biosensor based on the immobilization of horseradish peroxidase onto Au-modified titanium dioxide nanotube arrays *Biosensors and Bioelectronics*. **24**(4), 566 (2008).
- 128.L. Li, J. Huang, T. Wang, H. Zhang, Y. Liu and J. Li: An excellent enzyme biosensor based on Sb-doped SnO₂ nanowires *Biosensors and Bioelectronics*. **25**(11), 2436 (2010).
- 129.H.W. Pickering, and P.R. Swann: Electron metallography of chemical attack upon some alloys susceptible to stress corrosion cracking. *Corrosion* **19**, 373 (1963).
130. H.W. Pickering, and C. Wagner: Electrolytic dissolution of binary alloys containing a noble metal. *Journal of the Electrochemical Society* **698**, 114 (1967).
131. A.J. Forty: Corrosion micromorphology of noble metal alloys and depletion gilding. *Nature* **282**, 597 (1979).
132. A. Wittstock, V. Zielasek, J. Biener, C.M. Friend, and M. Bäumer: Nanoporous gold catalysts for selective gas-phase oxidative coupling of methanol at low temperature. *Science* **327**, 319 (2010).

133. K. Sieradzki, N. Dimitrov, D. Movrin, C. McCall, N. Vasiljevic, and J. Erlebacher: The dealloying critical potential. *Journal of the Electrochemical Society* **149**, B370 (2002).
134. J. Snyder, K. Livi, and J. Erlebacher: Dealloying silver/gold alloys in neutral silver nitrate solution: porosity evolution, surface composition, and surface oxides. *Journal of the Electrochemical Society* **155**, C464 (2008).
135. J. Erlebacher: An atomistic description of dealloying porosity evolution, the critical potential, and rate-limiting behavior. *Journal of the Electrochemical Society* **151**, C614 (2004).
136. J. Snyder, and J. Erlebacher: Kinetics of crystal etching limited by terrace dissolution. *Journal of the Electrochemical Society* **157**, C125 (2010).
137. T. Fujita, P. Guan, K. McKenna, X. Lang, A. Hirata, L. Zhang, T. Tokunaga, S. Arai, Y. Yamamoto, N. Tanaka, Y. Ishikawa, N. Asao, Y. Yamamoto, J. Erlebacher, and M. Chen: Atomic origins of the high catalytic activity of nanoporous gold. *Nat Mater* **11**, 775 (2012).
138. J. Snyder, P. Asanithi, A. B. Dalton, and J. Erlebacher: Stabilized nanoporous metals by dealloying ternary alloy precursors. *Advanced Materials* **20**, 4883 (2008).
139. M. Hakamada, and M. Mabuchi: Mechanical strength of nanoporous gold fabricated by dealloying. *Scripta Materialia* **56**, 1003 (2007).
140. R. Morrish, K. Dorame, and A. J. Muscat: Formation of nanoporous Au by dealloying AuCu thin films in HNO₃. *Scripta Materialia* **64**, 856 (2011).
141. L.H. Qian, and M.W. Chen: Ultrafine nanoporous gold by low-temperature dealloying and kinetics of nanopore formation. *Applied Physics Letters* **91**, 083105 (2007).
142. Y. Ding, Y.J. Kim, and J. Erlebacher: Nanoporous Gold Leaf: "Ancient Technology"/Advanced Material. *Advanced Materials* **16**, 1897 (2004).

143. J. Biener, A.M. Hodge, J.R. Hayes, C.A. Volkert, L.A. Zepeda-Ruiz, A.V. Hamza, and F.F. Abraham: Size Effects on the Mechanical Behavior of Nanoporous Au. *Nano Letters* **6**, 2379 (2006).
144. E. Detsi, S. Punzhin, J. Rao, P.R. Onck, and J.T.M. De Hosson: Enhanced strain in functional nanoporous gold with a dual microscopic length scale structure. *ACS Nano* **6**, 3734 (2012).
145. H. Oppermann, and L. Dietrich: Nanoporous gold bumps for low temperature bonding. *Microelectronics Reliability* **52**, 356 (2012).
146. V. Zielasek, B. Jürgens, C. Schulz, J. Biener, M. M. Biener, A. V. Hamza, and M. Bäumer: Gold catalysts: nanoporous gold foams. *Angewandte Chemie International Edition* **45**, 8241 (2006).
147. G. Patrick, E. van der Lingen, C.W. Corti, R.J. Holliday, and D.T. Thompson: The potential for use of gold in automotive pollution control technologies: a short review. *Topics in Catalysis* **30-31**, 273 (2004).
148. T.V. Choudhary, and D.W. Goodman: Catalytically active gold: The role of cluster morphology. *Applied Catalysis A: General* **291**, 32 (2005).
149. G. J. Hutchings: Vapour phase hydrochlorination of acetylene: Correlation of catalytic activity of supported metal catalysts. *Journal of Catalysis* **96**, 292 (1985).
150. M. Haruta, T. Kobayashi, H. Sano, and N. Yamada: Novel gold catalysts for the oxidation of carbon monoxide at a temperature far below 0°C. *Chemistry Letters* **16**, 405 (1987).
151. C. Xu, J. Su, X. Xu, P. Liu, H. Zhao, F. Tian, and Y. Ding: Low temperature CO oxidation over unsupported nanoporous gold.. *Journal of the American Chemical Society* **129**, 42 (2007).

152. R. Zeis, T. Lei, K. Sieradzki, J. Snyder, and J. Erlebacher: Low temperature CO oxidation over unsupported nanoporous gold. *Journal of Catalysis* **253**, 132 (2008).
153. J. Zhang, P. Liu, H. Ma, and Y. Ding: Nanostructured Porous Gold for Methanol Electro-Oxidation. *The Journal of Physical Chemistry C* **111**, 10382 (2007).
154. Y. Deng, W. Huang, X. Chen, and Z. Li: Facile fabrication of nanoporous gold film electrodes. *Electrochemistry Communications* **10**, 810 (2008).
155. L.C. Nagle, and J.F. Rohan: Nanoporous Gold Catalyst for Direct Ammonia Borane Fuel Cells. *Journal of the Electrochemical Society* **158**, B772 (2011).
156. L.C. Nagle, and J.F. Rohan: Nanoporous gold anode catalyst for direct borohydride fuel cell. *International Journal of Hydrogen Energy* **36**, 10319 (2011).
157. X. Yan, F. Meng, S. Cui, J. Liu, J. Gu, and Z. Zou: Effective and rapid electrochemical detection of hydrazine by nanoporous gold. *Journal of Electroanalytical Chemistry* **44**, 661 (2011).
158. B. K. Jena, and C.R. Raj: Ultrasensitive nanostructured platform for the electrochemical sensing of hydrazine. *The Journal of Physical Chemistry C* **111**, 6228 (2007).
159. F. Meng, X. Yan, J. Liu, J. Gu, and Z. Zou: Nanoporous gold as non-enzymatic sensor for hydrogen peroxide. *Electrochimica Acta* **56**, 4657 (2011).
160. K. Twomey, L. C. Nagle, A. Said, F. Barry, and V.I. Ogurtsov: Characterisation of Nanoporous Gold for use in a dissolved oxygen sensing application. *BioNanoScience* **5**, 55 (2015).
161. N.A. Mohd Said, V.I. Ogurtsov, K. Twomey, L.C. Nagle, and G. Herzog: Chemically Modified Electrodes for Recessed Microelectrode Array. *Procedia Chemistry* **20**, 12 (2016).

162. C.A.R. Chapman, H. Chen, M. Stamou, J. Biener, M.M. Biener, P.J. Lein, and E. Seker: Nanoporous Gold as a Neural Interface Coating: Effects of Topography, Surface Chemistry, and Feature Size. *ACS Applied Materials & Interfaces* **7**, 7093 (2015).
163. D.V. Pugh, A. Dursun, and S.G. Corcoran: Formation of nanoporous platinum by selective dissolution of Cu from Cu_{0.75}Pt_{0.25}. *Journal of Materials Research* **18**, 216 (2003).
164. L.-Y. Chen, J.-S. Yu, T. Fujita, and M.-W. Chen: Nanoporous copper with tunable nanoporosity for SERS applications. *Advanced Functional Materials* **19**, 1221 (2009).
165. M. Hakamada, J. Motomura, F. Hirashima, and M. Mabuchi: Preparation of Nanoporous Ruthenium Catalyst and Its CO Oxidation Characteristics. *Materials Transactions* **53**, 524 (2012).
166. Q. Chen, and K. Sieradzki: Spontaneous evolution of bicontinuous nanostructures in dealloyed Li-based systems. *Nat. Mater.* **12**, 1102 (2013).
167. P. Vazquez, G. Herzog, C. O'Mahony, J. O'Brien, J. Scully, A. Blake, C. O'Mathuna, and P. Galvin: Microscopic gel-liquid interfaces supported by hollow microneedle array for voltammetric drug detection. *Sensors and Actuators B: Chemical* **201**, 572 (2014)

Table 1. Summary of GOx functionalized 1D metal/metal oxide nanostructure based glucose sensors.

Electrodes	Sensitivity ($\mu\text{A mM}^{-1} \text{cm}^{-2}$)	Linear range (mM)	LOD (μM)	References
Ag NWs/GOx	-	0.01 – 0.8	2.83	68
AuNP-Pb/GOx NWs array	135.5	0.005 – 2.2	2	69
Au/GOx NWs	-	0.01 – 20	5	70
Au/GOx tube arrays	0.4	10 – 20	-	71
Au/GOx nanoelectrode arrays	40	28-65	0.0124	72
Au-Ni nanorod arrays	769.5	0.275 – 27.5	5.5	76
Au/Ag-GOx nanorods	34.29	2 - 12	-	77
Pt/CNT-GOx	-	0.16-11.5	0.55	73
C-ZnO/GOx NWs Array	35.3	0.01 – 1.6	1	74
ZnO/Au-GOx NWs	19.5	0.2 - 2	50	75
Pt-GOx NWs	30	0.05 – 0.15	3	64
TiO ₂ -GOx nanorods	0.232	0.05 – 1.32	2	78
N-TiO ₂ /GOx nanotube array	733.17	0.05 – 0.85	2.9	79
Au-V ₂ O ₅ -GOx NWs	-	0 - 0.1	0.5	80
Au/ZnO-GOx nanorods	1492	0.001 – 0.33	0.1	81
ZnO-GOx nanorods	-	0.03 – 0.3	3	82
ZnO-GOx nanotube arrays	30.85	0.1 – 4.2	10	83
ZnO-GOx NWs	26.3	0.001 – 0.76	0.7	84
Pd/C-GOx nanofiber	13	0.06 – 6	3	85
CeO ₂ -GOx nanorods	0.165	2 - 26	100	86
PANI nanotubes	97.18	0.01 – 0.5	0.3	87

*NWs – Nanowires, *GOx-Glucose Oxidase, *C-Carbon, *N-Nitrogen, *PANI - Polyaniline

Table 2: Summary of recently developed non-enzymatic glucose biosensor based on 1D array nanostructures.

Electrodes	Sensitivity ($\mu\text{A mM}^{-1} \text{cm}^{-2}$)	Linear range (mM)	LOD (μM)	References
Au NWs Array	309	1 – 10	50	90
Ultrathin Au NWs	56	0 - 12	20	89
Au NWs	-	0.4 – 10	0.036	91
Pt-Pb NWs arrays	11.25	0 – 11	8	92
Pt-Ni NWs	40	0.002 - 2	1.5	93
Pt nanotube	0.1	2 - 14	1	94
Pt-Pd nanotube arrays	41.5	0.1 - 10	-	95
Pt-Pd nanowire arrays	27.6	0.1 - 10	-	95
Ni NWs Array	1043	3×10^{-4} - 7	0.1	96
Pt-Ni NWs Array	96	1 - 8	83	97
NiO@Ni NWs Array	170	1-7	14	98
Ni NWs array	4243	0.003 - 2	0.1	99
Cu NWs	420.3	0.001 - 2	0.35	100
Ni(OH) ₂ -TiO ₂ nanotube	120	0.02 – 1.7	5	101
Ni/NiTiO ₃ /TiO ₂ nanotube arrays	456.4	0.005 – 0.5	0.7	102
Ti/TiO ₂ -Ni nanotube arrays	200	0.1 – 1.7	4	103
Ni-Cu NWs	1600	0.0001 – 1.2	0.1	104
Cu ₂ O/TiO ₂ nanotube arrays	14.56	3 - 9	62	105
Ni-TiO ₂ nanotubes	700.2	0.004 – 4.8	2	106
CuO nanowire arrays	1420.3	upto 2.55	5.1	107
Ni NWs	367	0.01 - 5	1	108
Fe ₂ O ₃ nanowire arrays	726.9	0.015 - 8	6	109
CuO/Cu NWs	-	upto 2	0.49	110
FeOOH nanowire	12.13	0.15 – 3	-	111

*NWs – Nanowires

Table 3. Summary of typical H₂O₂ biosensors with the 1D array nanostructure in both enzyme and non-enzyme systems.

Electrodes	Sensitivity ($\mu\text{A mM}^{-1} \text{cm}^{-2}$)	Linear range (mM)	LOD (μM)	References
Ag NWs	4705	0.5 – 10.35	10	115
Ag NWs array	2.66	0.1 – 3.1	29.2	116
Ag/MnOOH nanorods	32.57	0.05 – 12.8	1.5	121
Au films	-	0.1 – 8	3.26	122
Au NWs	-	0.05 – 22.65	30	117
Pd-Au NWs array	530	upto 2	5	118
Au-MnO ₂ nanorods	980	0.022 – 12.6	0.05	123
Au-Si NWs array	-	0.2 – 1	-	124
CuO/Si NWs	22.270	0.01 – 13.18	1.6	119
Pd/C nanofibers	315	0.005 – 2.1	3	85
Pt/Au NWs array	194.6	0.02 - 20	1	97
Pt/CNT-TiO ₂ nanotubes	0.134	0.001 - 2	1	125
Pt/CNT nanotubes	-	0.005 – 0.25	1.5	73
Pt-Au/TiO ₂ nanotubes	2.92	0.01 – 0.08	10	126
HRP/C-ZnO NWs array	237.8	upto 4	0.2	74
HRP/Au NWs array	45.86	upto 15	0.42	120
HRP/Au-ZnO nanorods	36.28	0.005 – 1.7	1.9	127
HRP/Au-TiO ₂ nanotubes	-	0.005 – 0.4	2	128
HRP/Sb-SnO ₂ nanowires	100	0.01 – 0.45	0.8	129

*NWs – Nanowires, CNT-Carbon Nanotube, C- Carbon, HRP – Horseradish Peroxidase

FIG. 1. Potentiostat connected to three electrode cell, and corresponding schematic (reproduced from Ref 16)

FIG. 2. Modern Day Potentiostats (reproduced from Ref 16)

FIG. 3. HeLa cells growing on gold nano-pillars fabricated on an interdigitated impedance gold electrode.³⁴

FIG. 4. SEM images of different metal/metal oxide nanowire structures (a) TiO₂ nanorods (Reproduced from Yang et al.)⁷⁸, (b) ZnO nanorods (Reproduced from Liu et al.)⁸², (c) Pt nanowire (Reproduced from Qu et al.)⁶⁴ and (d) Au nanowire (Reproduced from Liu et al.)⁷⁰

FIG. 5. SEM images of Ni nanowire structures (a) Ni NWs fabricated by electrodeposition using Polycarbonate (PC) template (Reproduced from Lu et al.),⁹⁵ (b) Pt-Ni NWs arrays (Reproduced from Jamal et al.)⁹⁶, (c) NiO@Ni nanowire by electrodeposition using AAO template (Reproduced from Jamal et al.)⁹⁷ and (d) Ni NWs electrodeposited using AAO template (Reproduced from Jamal et al.)⁹⁷

FIG. 6. Amperometric interferences current response curves of (a) Pt-Ni NWs array sensor (Reproduced from Ref 97) and (b) NiO@Ni NWs array glucose sensor (Reproduced from Ref 98)

FIG. 7. (a) SEM and (b) TEM images showing cross sectional view of nanoporous gold formed by dealloying gold-silver alloy in nitric acid, showing typical ligament and pore dimensions..

FIG. 8. Linear sweep voltammograms for oxidation of (a) ammonia borane and (b) sodium borohydride at the gold electrodes investigated recorded at 10 mV/s for 20 mM solutions of borane or borohydride in 1 M NaOH. The oxidation responses at nanoporous gold are shown in blue, while the responses at the gold nanowire and planar gold disc electrodes are shown in red and green, respectively.

FIG. 9 SEM images of (a) unmodified recessed gold micro-disc array (b) individual unmodified recessed gold micro-disc (c) recessed gold micro-disc array modified with AuAg alloy (d) NPG-modified recessed micro-disc array, (e)-(f) individual NPG-modified micro-disc (g) side wall of an unmodified recessed gold micro-band (h) NPG-modified recessed gold micro-band array (i) sidewall view of a NPG-modified recessed gold micro-band. Images were recorded at 30 kV with a 60° tilt.

FIG 1.

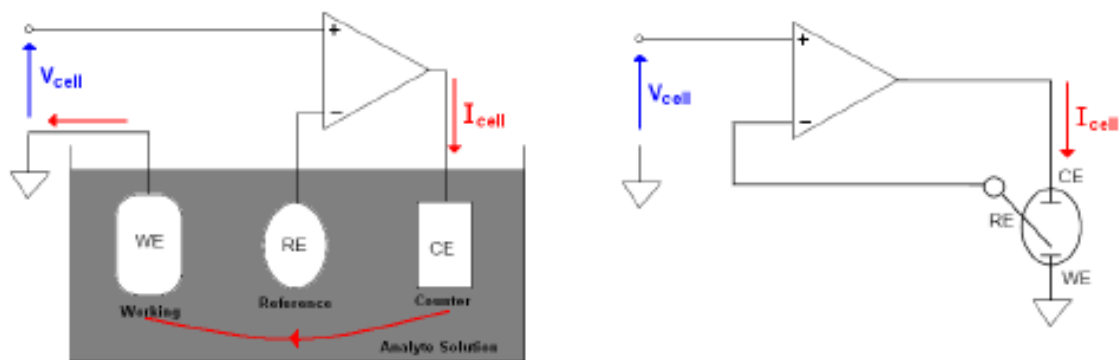


FIG 2

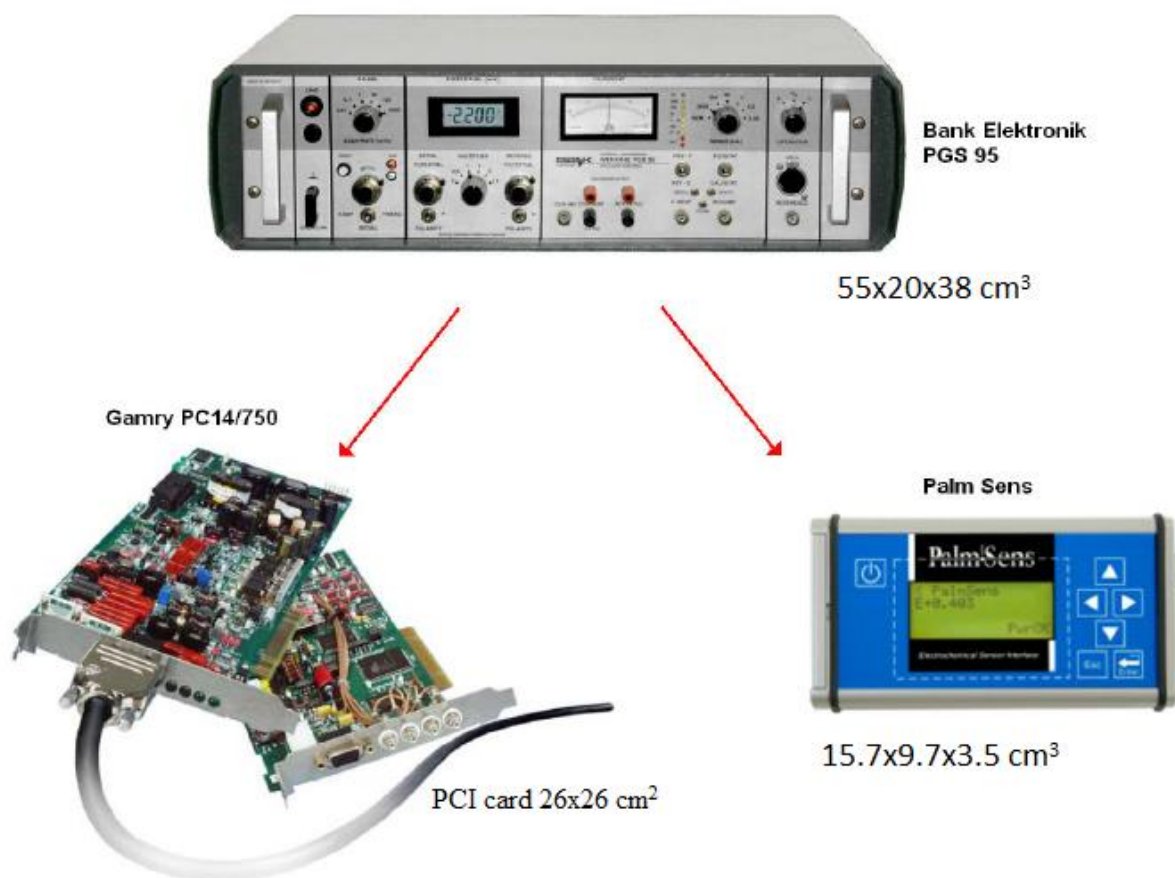


FIG 3

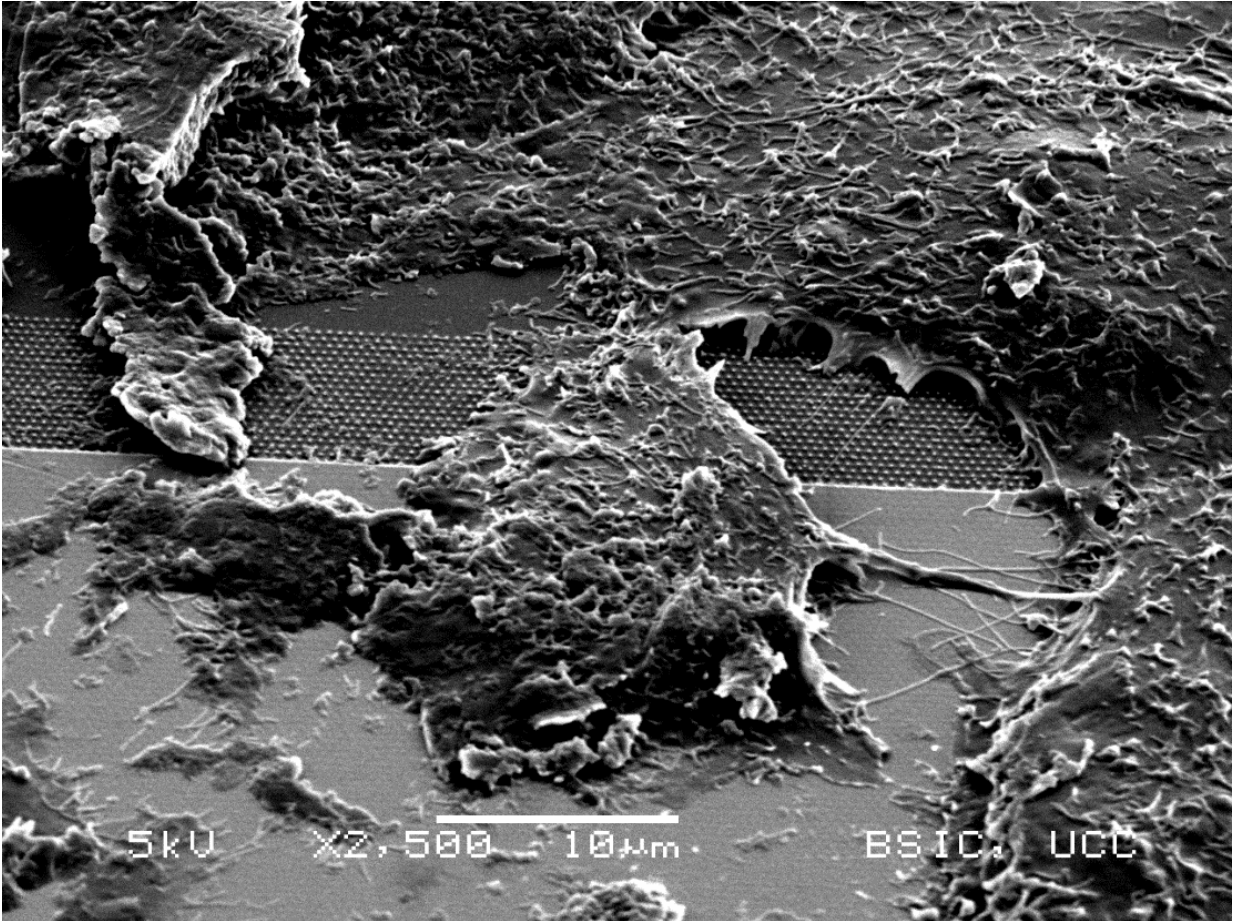


FIG 4

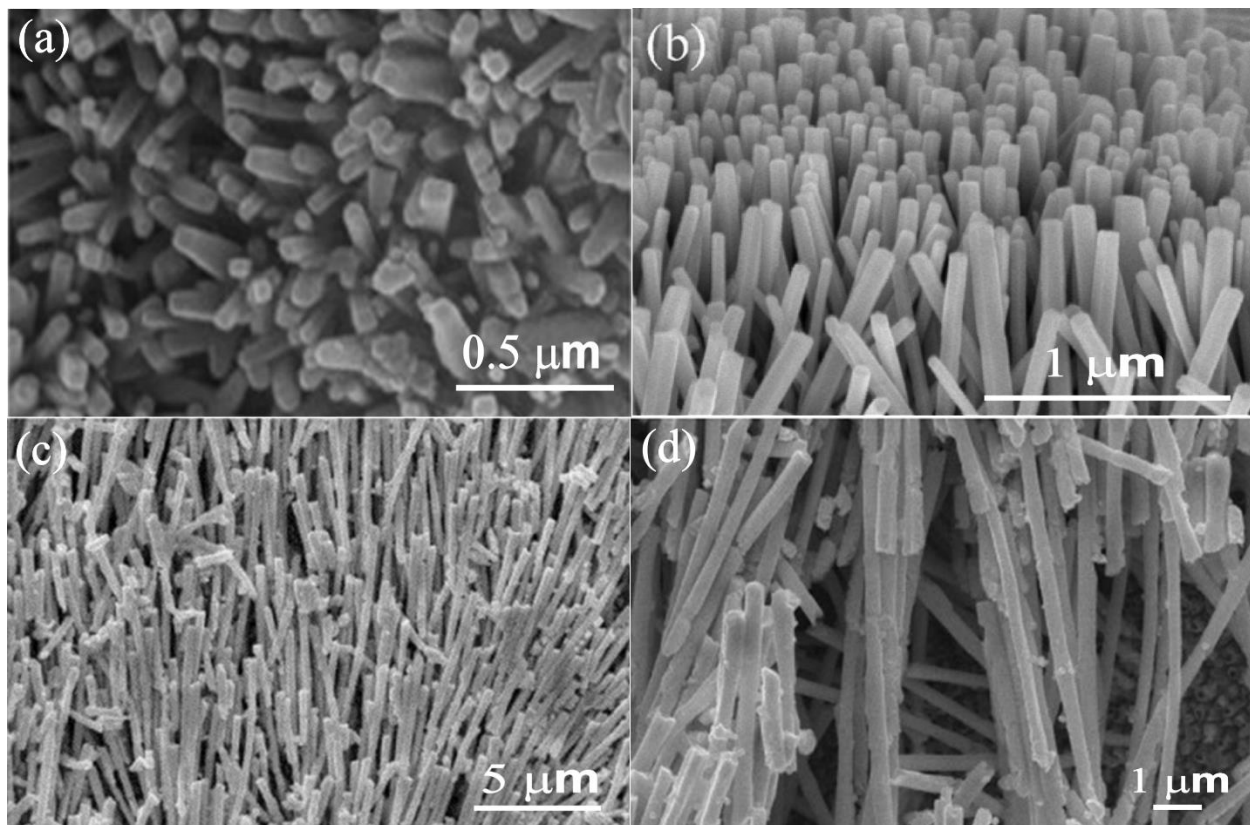


FIG 5

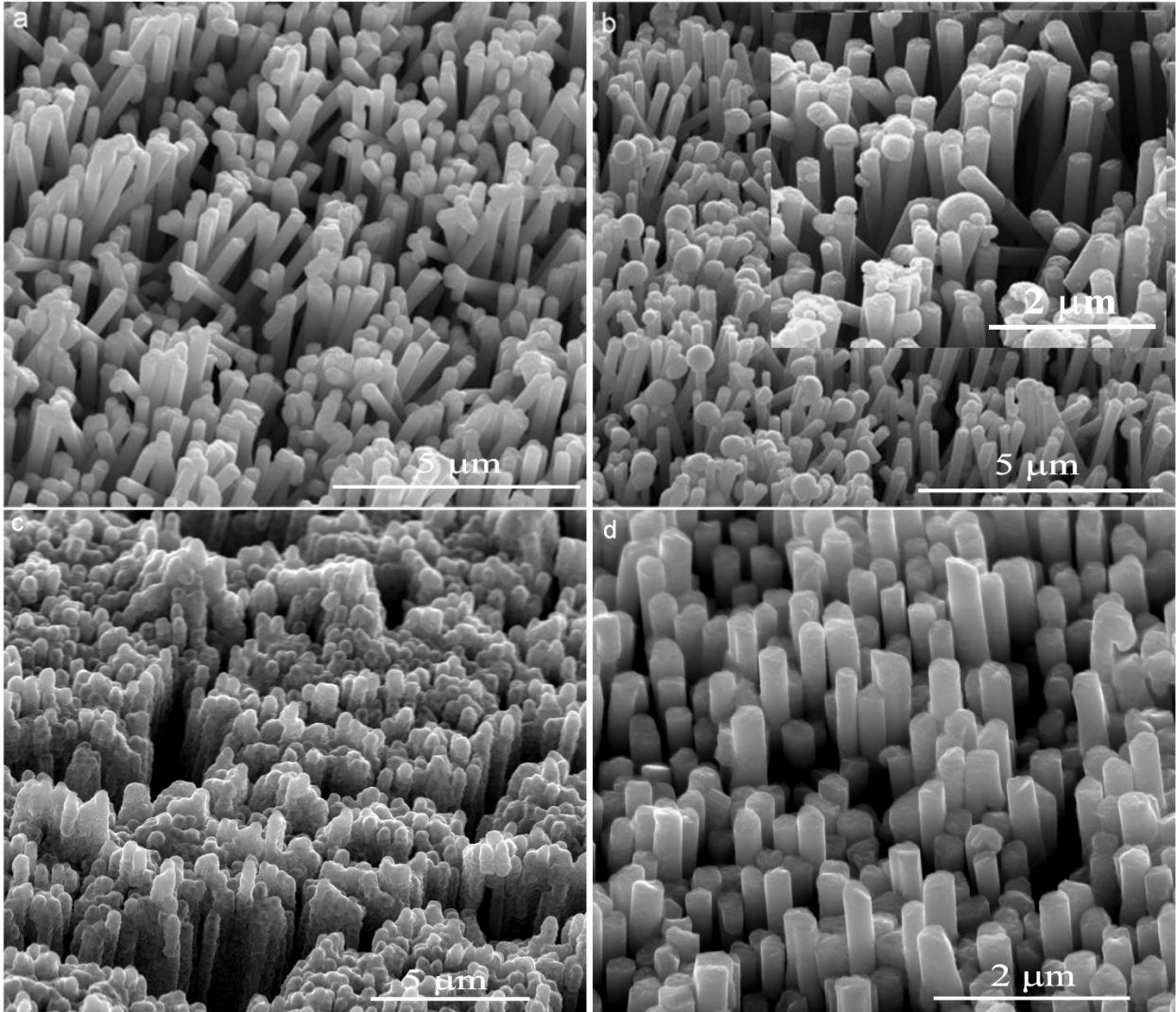


FIG 6

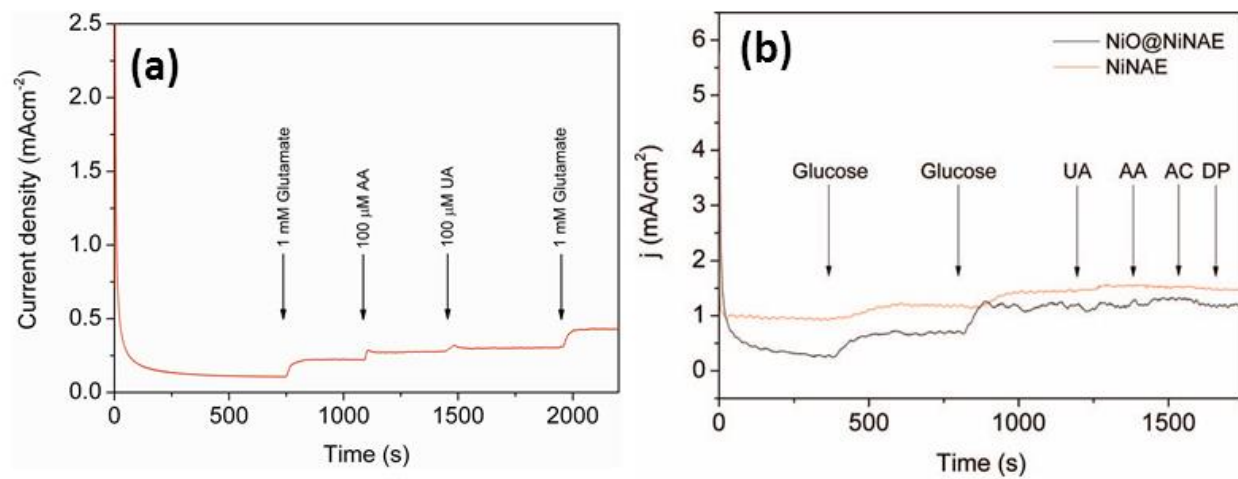


FIG 7

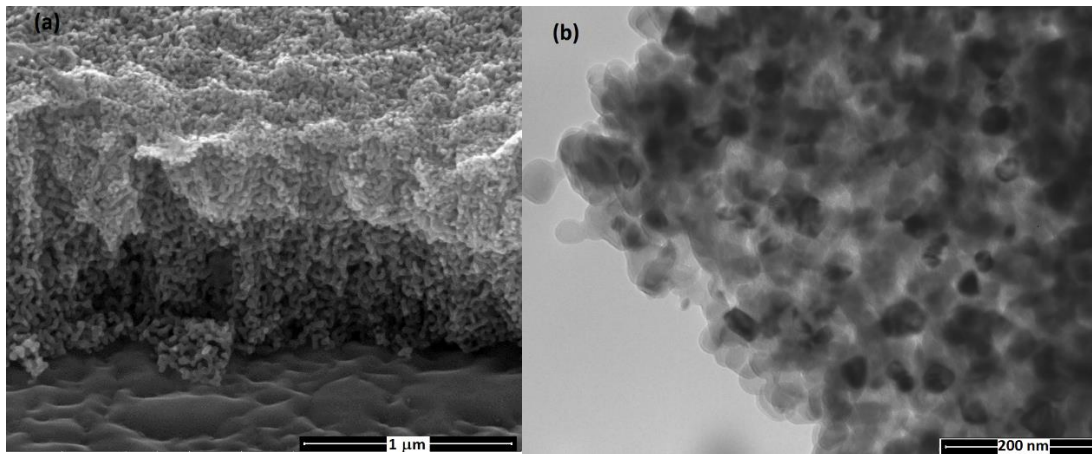


FIG 8

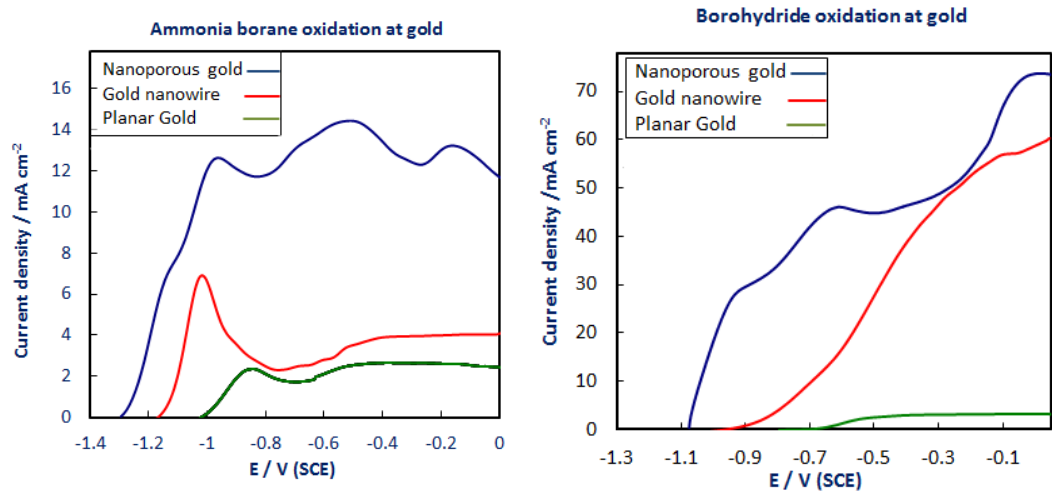
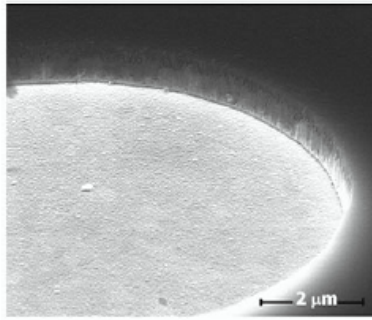
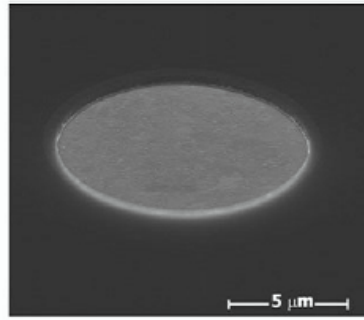


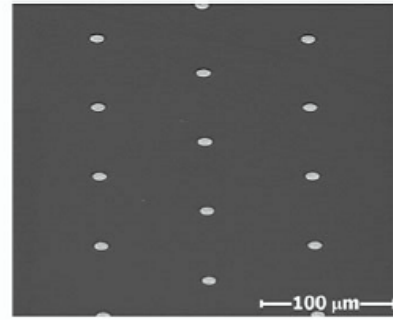
FIG 9



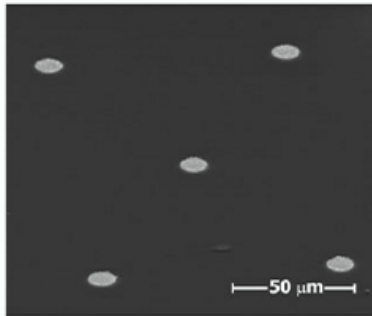
(a)



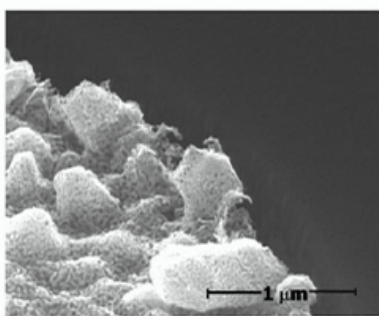
(b)



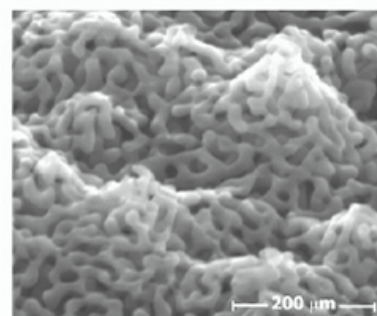
(c)



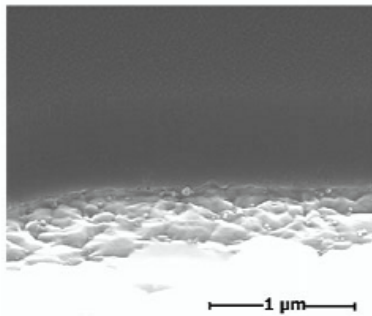
(d)



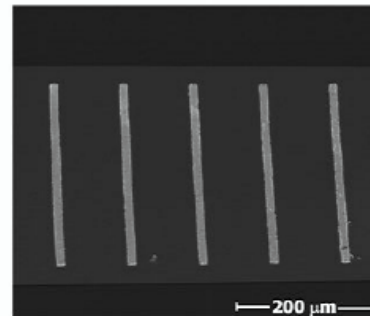
(e)



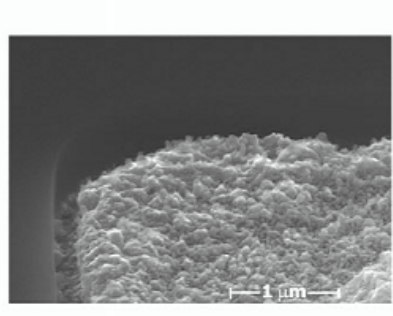
(f)



(g)



(h)



(i)